

SHRP-P-688

# **SHRP-LTPP Data Analysis Studies: Five-Year Report**

William O. Hadley  
Hadley and Associates



**Strategic Highway Research Program**  
National Research Council  
Washington, DC 1994

SHRP-P-688  
Product no. 5000

Program Manager: *Neil F. Hawks*  
Five-Year Report Manager: *A. Robert Raab*  
Program Manager: *A. Robert Raab*  
Program Area Secretaries: *Cynthia Baker, Francine A. Burgess*  
Production Editor: *Margaret S. Milhous*

July 1994

key words:  
AASHTO design equations  
data analysis  
empirical analysis  
load equivalence factor  
mechanistic analysis  
rutting  
sensitivity analysis  
servicability loss

Strategic Highway Research Program  
National Research Council  
2101 Constitution Avenue N.W.  
Washington, DC 20418

(202) 334-3774

The publication of this report does not necessarily indicate approval or endorsement of the findings, opinions, conclusions, or recommendations either inferred or specifically expressed herein by the National Academy of Sciences, the United States Government, or the American Association of State Highway and Transportation Officials or its member states.

NAP/450M/794

## Acknowledgments

The research described herein was supported by the Strategic Highway Research Program (SHRP). SHRP is a unit of the National Research Council that was authorized by section 128 of the Surface Transportation and Uniform Relocation Assistance Act of 1987.

The authors/editors of this report are Dr. William O. Hadley, Dr. Virgil Anderson, Mr. Jonathan Groeger, and Mr. Charlie Copeland. All authors were associated with Texas Research and Development Foundation (TRDF) during the Long-Term Pavement Performance program. Contributions by Mr. Gonzalo Rada of PCS/Law, Mr. Amir Hanna of SHRP and Dr. Shiraz Tayabji of PCS/Law, and Dr. Brent Rauhut of Brent Rauhut Engineering Inc. (BRE) and Dr. Gilbert Baladi of Michigan State University are gratefully recognized. The manuscript was prepared by Ms. Jan Zeybel.

The publication of this report does not necessarily indicate approval or endorsement by the National Academy of Sciences, by the Federal Highway Administration, or by any state highway or transportation department of the findings, opinions, conclusions, or recommendations either inferred or specifically expressed herein.

# Contents

Acknowledgments .....	iii
List of Tables .....	vii
List of Figures .....	ix
Data Analysis Studies for the SHRP-LTPP Program .....	1
Background .....	1
Introduction .....	2
An Approach to Improvements of LEFs from SHRP-LTPP Data .....	3
Introduction .....	3
Definition of LEF .....	3
Uses for LEF .....	4
Derivation of LEFs .....	5
Analytical Implications of SHRP-LTPP Database LEFs .....	5
Approach to Calculation of Alternative LEFs and ESALs from LTPP Traffic Data .....	6
AASHTO Road Test PSI Relationships .....	8
Flexible Pavement .....	12
Rigid Pavement .....	12
SHRP-LTPP Approach to LEF Evaluation .....	12
LEF Evaluation Techniques .....	13
Rigid Pavement LEF Evaluation .....	13
Evaluation of log(IRI) .....	15
Evaluation of log(PSI-Loss) .....	15
Regional Aspects of Rigid Pavement Performance .....	20
Possible Effects on LEF Values for Rigid Pavements .....	20
Flexible Pavement LEF Evaluation .....	24
Evaluation of Rutting .....	26
Evaluation of Roughness (IRI) .....	26
Evaluation of AASHTO Serviceability Loss .....	31
Evaluation of SHRP Serviceability Loss [ $\{K/(1-K)\}(p_n-2.0)$ ] .....	31
Conclusions and Recommendations .....	34

Materials and Construction Variability Study .....	37
Approach .....	37
Construction Variability in Rigid Pavement .....	37
Rigid Pavement Construction Variability Factors .....	37
Longitudinal Roughness in Rigid Pavements, log(IRI) .....	43
AASHO Serviceability Loss .....	44
Construction Variability in Flexible Pavements .....	45
Flexible Pavement Construction Variability Factors .....	45
log(Layer Rutting) .....	45
log(Deep Rutting) .....	49
AASHO Serviceability Loss .....	50
Conclusions .....	51
 Rutting Initiation Studies .....	 53
Introduction .....	53
Rut Depth Estimation and Cross Profile Distortion .....	53
Introduction .....	53
Analytical Approach .....	54
Selected SHRP-LTPP Sections .....	57
Type of Rutting .....	62
Rut Predication Equations .....	70
Applications .....	73
SHRP Data Analysis Contract: Brent Rauhut Engineering Inc. and ERES Consultants Inc. (P-020) .....	76
Introduction .....	76
Limitations Resulting from Data Shortcomings .....	77
Sensitivity Analyses and Results .....	78
Summary of Sensitivity Analysis Results for HMAC Pavements .....	80
Summary of Sensitivity Analysis Results for PCC Pavements .....	84
Evaluation of the AASHTO Flexible Pavement Design Equation .....	87
Evaluation of the AASHTO Rigid Pavement Design Equation .....	90
Evaluation of the 1993 AASHTO Overlay Design Equations .....	94
Recommendations for Future Analyses .....	95
SHRP Data Analysis Contract: Michigan State University (P-020B) .....	97
Premises of the AASHTO Design Procedure for Flexible Pavements .....	98
Mechanistic Evaluation/Calibration of the AASHTO Design Procedure ...	98
 References .....	 101

## List of Tables

Table 1	Exponents for Approximation of AASHO LEFs by the Load Ratio Function . . . . .	9
Table 2	Flexible and Rigid Pavement Sections Included in the LEF Study . . . . .	14
Table 3	Structural and Environmental Factors - Rigid Pavement Sections . . . . .	16
Table 4	Estimates for Rigid Sections . . . . .	17
Table 5	Regression Analysis Results, log(IRI), for Rigid Pavement Analysis . . . . .	19
Table 6	Regression Analysis Results, log(4.2-PSI) for Rigid Pavement Analysis . . . . .	21
Table 7	log(IRI) for PCC Jointed Pavements . . . . .	22
Table 8	log(4.2 - PSI) for PCC Jointed Pavements . . . . .	23
Table 9	Environmental and Structural Information for Flexible Pavement Sections . . . . .	25
Table 10	Traffic Estimates for Flexible Sections . . . . .	27
Table 11	Regression Analysis Results, log(RUT), Flexible Pavement Analysis . . . . .	29
Table 12	Regression Analysis Results - AASHO Serviceability Loss Flexible Pavement Analysis . . . . .	30
Table 13	Regression Analysis Results - SHRP Serviceability Loss Flexible Pavement Analysis . . . . .	33
Table 14	Possible LEF Changes Identified in This Study . . . . .	35
Table 15	Site Specific Information and Data - Rigid Pavement Construction Variability Study . . . . .	41
Table 16	Site Specific Information and Data - Flexible Pavement Construction Variability Study . . . . .	46
Table 17	List of LTPP Sections for the Flexible Pavement Structures . . . . .	59
Table 18	List of LTPP Sections for the Composite Pavement Sections . . . . .	61
Table 19	Rut Type Combinations - HMAC on Stabilized Base . . . . .	65
Table 20	Rut Type Combinations - HMAC on Granular Base . . . . .	67
Table 21	HMAC Overlay of HMAC . . . . .	69
Table 22	Coefficients of Regression Equations Developed to Predict Rutting in HMAC on Granular Base for the Wet-Freeze Dataset . . . . .	79
Table 23	Sensitivity Analysis Results: HMAC . . . . .	83
Table 24	Sensitivity Analysis Results: PCC . . . . .	85
Table 25	Results from Comparative Evaluation of 1993 AASHO Overlay Equations . . . . .	96

## List of Figures

Figure 1	Power Function Approximations to AASHTO Flexible Pavement LEFs when SN = 5	10
Figure 2	Power Function Approximations to AASHTO Rigid Pavement LEFs when PCC Thickness = 10"	11
Figure 3	Construction Variability Factors	38
Figure 4	Distress Prediction Model	39
Figure 5	Actual Analytical Approach	40
Figure 6	Example of Intermediate Point to Higher Elevation Between Starting Point (X5) and Ending Point (X14) of a Straightedge	55
Figure 7	Pavement Distortion Possibilities	56
Figure 8	Environmental Zones for SHRP-LTPP Experiments	58
Figure 9	Source of Rutting - HMAC on Stabilized Base	63
Figure 10	Source of Rutting on Granular Bases	66
Figure 11	Source of Rutting - HMAC Overlay of HMAC	68
Figure 12	Rut Depth Regression Equations - HMAC on Granular Base	71
Figure 13	Rut Depth Equations - HMAC on Stabilized Base	72
Figure 14	Rut Depth Equations - HMAC Overlay of HMAC	74
Figure 15	Rut Depth Equations - HMAC Overlay of PCC	75
Figure 16	Results of Sensitivity Analysis for Rutting in HMAC Granular Base	81
Figure 17	Results of Sensitivity Analysis for Rutting in HMAC on Granular Base	82
Figure 18	Predicted KESALs versus Actual KESALs for JPCP and PRCP Using Original AASHTO Prediction Models	92
Figure 19	Predicted KESALs versus Actual KESALs for JPCP, JRCP, and CRCP Using 1993 AASHTO Prediction Models	93

# Data Analysis Studies for the SHRP-LTPP Program

## Background

One of the principal objectives of the Strategic Highway Research Program Long-Term Pavement Performance (SHRP-LTPP) study was the development of a comprehensive electronic media database for housing pavement performance data covering a wide range of conditions and service life factors (1). The database was structured to address pavement management and engineering design issues including:

- Pavement rehabilitation design and construction procedures
- Effects of pavement maintenance
- Cost of deferred maintenance
- Climatic and environmental effects
- Long-term load effects
- Validity of the American Association of State Highway and Transportation Officials (AASHTO) Road Test load equivalency factors (LEFs)
- Relative effects and interactions of load, environmental conditions, and materials properties
- Effects of subgrade material
- Load carrying capacity beyond pavement design life
- Effects of alternative drainage designs (1)

The extent and scope of information contained within the LTPP database and Information Management System (IMS) also provides the resources not only to evaluate or revise existing design equations but to develop new ones.

A more specific research plan was developed for the LTPP program with the stated goal "to increase pavement life by investigation of various designs of pavement structures and rehabilitated pavement structures, using different materials and under different loads, environments, subgrade soil and maintenance practices" (2). In this effort six specific objectives were established:

1. To evaluate existing design methods
2. To develop improved design methods and strategies for pavement rehabilitation
3. To develop improved design equations for new and reconstructed pavements
4. To determine the effects of load, environment, materials properties, variability, construction quality, and maintenance levels on pavement distress and performance

5. To determine the effects of specific design features on pavement performance
6. To establish a national long-term pavement performance database to support SHRP objectives and future needs

## **Introduction**

During the first 5 years of the SHRP-LTPP program most, if not all, of these issues and objectives were addressed in various SHRP-LTPP data analysis studies. For instance, the principal SHRP technical assistance contract (P-001) involved data analysis related to construction variability (Objective 4), SHRP LEF approach (Objective 5), and pavement rutting (Objective 4).

In addition, the principal SHRP data analysis contract (P020A) involved data analysis activities related to evaluation of existing design methods (Objective 1), improved design equations (Objective 3), effects of load and environment on pavement distress and performance (Objective 4), and effects of specific design features on pavement performance (Objective 5). A second SHRP data analysis contract (P020B) represented an initial effort to evaluate the AASHTO design equations in light of mechanistic-empirical analysis techniques. Another SHRP contract (H-101) was undertaken to assess the effectiveness of six pavement maintenance treatments, in response to Objective 2.

Several contracts, not directly associated with the SHRP-LTPP program, also pursued research activities related to the LTPP goals. The Canadian Strategic Highway Research Program (CSHRP-LTPP) explored high-risk research aimed at developing procedures to determine the cost-effectiveness of rehabilitation alternatives. The University of Birmingham (United Kingdom) pursued two contracts related to a proposed approach for SHRP database analysis; one involving measurement of pavement life cycle cost sensitivity to traffic, materials, and maintenance and rehabilitation processes, and the second involving the development of network-level pavement performance models.

The SHRP-LTPP Overview Report should be consulted if the reader desires additional information concerning the overall LTPP Program (3).

Data analysis studies concerning LEFs, materials and construction variability, rutting initiation studies, and the results of the specific SHRP-LTPP data analysis contracts are presented in subsequent sections of this report. These studies represent initial efforts in pursuit of LTPP goals and objectives and are based primarily on early General Pavement Studies (GPS) data. More extensive data analysis studies will follow in the years to come.

# An Approach to Improvements of LEFs from SHRP-LTPP Data

## *Introduction*

The necessity for improved or enhanced LEFs was one of the questions posed in "American's Highways: Accelerating the Search for Innovation" (1). It was proposed that the impacts of varying pavement strengths (or structural support), pavement structures, material types and environments on the AASHO Road Test LEFs could be investigated in a comprehensive long-term pavement performance database such as SHRP-LTPP. This study was undertaken to define an approach (or approaches) which could subsequently be used to investigate LEFs, once the SHRP-LTPP database is substantially populated.

There is no doubt that improved, enhanced or expanded equivalency factors would provide a basis for justification of decisions on cost allocation, pavement management and maintenance and rehabilitation strategies particularly if the factors are specific to a particular distress and applicable to wider ranges of pavement structure and environmental conditions. To pursue this objective, it is essential that an approach be defined which utilizes the LTPP database in an assessment of improvements of LEF from SHRP-LTPP data. One important question in this matter is whether or not there is sufficient data within the SHRP-LTPP database to investigate distress specific equivalence factors?

## **Definition of LEF**

An understanding of the definition, use and derivation of a classic LEF is important in the development of LEFs from SHRP-LTPP data.

The classical LEF definition is related to axle load application ratios for:

1. Designated level of specific distress type (DL)
2. Vehicles with constant loading factors (LF)
3. Pavements with specified structural factors (SF)
4. Specific environmental conditions (EF)

The vehicle loading factors (LF) generally consist of axle weight; axle configuration; vehicle class; tire type, size, and pressure. The type of distress (D) could be serviceability rating (PSI), rut depth, roughness or cracking, while the structural factors (SF) might be the Structural Number (SN) for a flexible pavement or surface thickness (D) for a rigid pavement. The distress level (DL) could be a PSI of 2.0 or 2.5, an average rut depth of 3/4 inch, a specified International Roughness Index (IRI) roughness level, or specified % cracking within the wheelpaths (e.g., 25%). The environmental conditions (EF) would be defined at least by moisture (wet or dry), temperature (freeze or nonfreeze) and subgrade soil type (fine or coarse grained).

In development of the LEF definition the term  $N(XLF | DL, SF, EF)$  represents the number of cumulative axle load applications imposed by vehicles with fixed loading factors (XLF) observed when a specified type of distress (D) has reached a designated level (DL) on a pavement with specified structural factors (SF) exposed to constant environment conditions (EF).

In the analytical process a standard set of axle loading factors (SLF) must be defined for comparative purposes. For instance an 18k single axle could be designated as the standard axle load; however, the other associated load factors, such as vehicle type, vehicle speed, tire type and pressure must also be fixed at specified levels. A set of nonstandard loading factors (XLF) is then established which should differ only from the standard loading factors (SLF) in the axle type (single, tandem, tridem) and axle weight (other than 18 kips).

By classical definition (Equation 1) the load equivalence factor for the nonstandard loading factors (XLF) equals the ratio of the observed number of axle applications for the standard load factors (SLF) to the observed number of axle applications for the nonstandard load factors (XLF), when DL, SF, and EF are all fixed and specified levels.

$$LEF(XLF | DL, SF, EF) = \frac{[N(SLF | DL, SF, EF)]}{[N(XLF | DL, SF, EF)]} \quad \text{Equation 1}$$

## Uses for LEF

The LEF is the basic element used to aggregate mixed combinations of axle applications and associated load factors into an Equivalent Standard Axle Load factor applications (i.e., ESALs) as presented in Equation 2.

$$ESALs = [N(LF_1) * LEF(LF_1)] + [N(LF_2) * LEF_2] + \dots + [N(LF_k) * LEF(LF_k)]$$

or

$$ESALs = \sum_{i=1}^k [N(LF_i) * LEF(LF_i)] \quad \text{Equation 2}$$

where

ESALs = number of equivalent standard axle load applications,  
 $N(LF_i)$  = number of axle applications of a specific axle with load factors  $i$   
 $LEF(LF_i)$  = load equivalence factor for the specific axle with load factor combination  $i$ .

The LEF can also be used as a basis for assessing the relative pavement damage attributable to the vehicle utilizing relative equivalence factors i.e.,  $LEF_1, LEF_2, \dots, LEF_k$ . In other words a

higher LEF for a vehicle implies greater pavement damage attributable to that vehicle when compared with a vehicle with a lower LEF.

## Derivation of LEFs

In order to derive LEFs, it is essential that a comprehensive database be available which contains a sufficient number of combinations of vehicle load factors ( $\_LF$ ), pavement structural factors (SF) and environmental conditions (EF) for all distress types (D) and levels (DL) under consideration, as well as, the number of axle applications (N) related to each axle load factor. In each instance the distress (D) should be that directly attributable to the specific axle ( $\_LF$ ) traveling on a designated pavement structure (SF) exposed to specific environmental conditions (EF).

If sufficient information is available in the database for these variables/factors then distress specific prediction equations could be developed in the form

$$DL = f(N, \_LF, SF, EF) \qquad \text{Equation 3}$$

where

- DL = the level of a specific distress type
- N = cumulative applications of an axle with load factors,  $\_LF$
- $\_LF$  = axle load factors (axle weight axle configuration, vehicle class, tire type and pressure, etc.)
- SF = pavement structural factors, SN, D, etc.
- EF = environmental conditions (wet-dry, freeze-nonfreeze; fine or coarse grained subgrade soils, etc.)

To develop LEFs from distress specific predictive relationships, the number of axle applications for a set of standard load factors, N(SLF) and sets of nonstandard load factors, N(XLF) must be determined from Equation 3 for all desired combinations of distress levels (DL), pavement structural factors (SF) and environmental conditions (EF). The LEFs for the nonstandard load factors (XLF) are then established by dividing N(SLF) by N(XLF) for each combination of distress level (DL), pavement structure (SF) and environmental conditions (EF).

## Analytical Implications of SHRP-LTPP Database LEFs

The AASHO LEFs were developed from the AASHO Road Test where carefully controlled and monitored traffic with fixed individual vehicle load factors (i.e., a specified particular vehicle type of constant tire type and pressure, axle configuration and loading) was maintained on each separate test loop composed of a number of constructed pavement structural sections.

The AASHO serviceability based LEFs (i.e., based on terminal PSI values of 2.0 and 2.5), were developed from the classical definition (Equation 1) for specific vehicle load factors, accurately measured vehicle axle applications, and specific localized environmental conditions. Since the AASHO Road Test included the assignment of specific vehicle types with constant load factors to the test loops, the damage (i.e., serviceability loss) could be directly attributable to the specific vehicle load factors for specific structures and environmental conditions.

The SHRP-LTPP database, on the other hand, is composed of observed and/or measured data and information obtained for a number of in-service highways of differing ages, pavement structures, construction variability and quality; exposed to mixed, and largely unknown, traffic; located in a variety of environmental zones; and displaying varying serviceability/distress levels. The traffic factors are particularly vexing since the traffic stream includes a wide variety of vehicle types (e.g., cars, trucks, 18 wheelers, etc.), axle configurations and loads, tire type and pressures. There is, therefore, no way to attribute the observed distress (or any portion of the observed distress) to a specific set of load factors. The total distress observed is, in fact, an accumulation of the distresses produced by the traffic stream. Since there is no way to separate the observed distress into portions attributable to each vehicle in the traffic stream, the distress specific prediction equations (Equation 3) and classical load equivalence factors (Equation 1) cannot be derived from SHRP-LTPP data.

### **Approach to Calculation of Alternative LEFs and ESALs from LTPP Traffic Data**

Since equations for distress associated with specific axle loadings (Equation 3) cannot be derived from the LTPP mixed traffic data, there is no direct basis for calculating the LEFs (Equation 1) and ESALs (Equation 2) that are needed for the derivation of distress prediction equations from the LTPP data.

One way to resolve this dilemma is to use LEFs (and resultant ESALs), that are presented in Appendix D of the AASHTO Design Guide (4) for all derivations that are ESAL dependent. The trouble with this method is that the AASHTO LEFs are strictly related to the PSI distress variable; whereas, LTPP analyses will often be needed for other distress variables. Moreover, if LEFs are sensitive to climatic changes, the AASHTO LEFs may not apply to other than the wet-freeze climates for LTPP sections.

For the purposes of this exploratory study, the methods described below was used to develop a family of LEF's (and resultant ESALs) whose elements include, in a well-defined manner, not only the AASHTO LEFs but also ranges about the AASHTO values. As discussed in later sections, the alternative ESALs were tested for their relative predictive value in the derivation of LTPP distress prediction equations.

The development of alternative LEFs (and ESALs) began with Equation 4 which specifies a mathematical form and other details related to Equation 3. By assumption, the attained level

(DL) of a specified distress variable (D) is considered to be satisfactorily predicted by the relationship

$$DL = A_0 N^{A_1} (L_1)^{A_{21}} (L_2)^{A_{22}} (S_1)^{A_{31}} (S_2)^{A_{32}} \dots (E_1)^{A_{41}} (E_2)^{A_{42}} \dots \quad \text{Equation 4}$$

where N is the number of applications of a load axle whose total weight is  $L_1$  (Kips) and whose number of component axles is  $L_2$ . Thus  $L_2$  would be 1 for single axles, 2 for tandem axles, 3 for tridem, and 4 for quadrem. All N applications are for a fixed combination of  $L_1$  and  $L_2$  and have been applied to a specified pavement section whose structural factors are  $S_1, S_2, \dots, S_n$ . The structural factors might include structural number for flexible pavements, layer thicknesses, layer moduli, etc. All applications would have occurred within climatic conditions represented by the factors  $E_1, E_2, \dots, E_n$ .

It is expected that the exponents  $A_1$  and  $A_{21}$  are positive since distress increases with number of applications (N) and increasing axle load ( $L_1$ ). The exponent  $A_{22}$  is expected to be negative with increasing  $L_2$  since the total axle load ( $L_1$ ) is spread out with increasing number of axles,  $L_2$ . If the structural factors ( $S_i$ ) increase with load-carrying capacity, the exponents  $A_{31}, A_{32}, \dots$  are expected to be negative and would thus produce decreasing distress as structural factor levels increase. The exponents  $A_{41}, A_{42}, \dots$ , are expected to be positive if the variables  $E_1, E_2, \dots, E_n$ , increase with climatic adversity to pavement performance.

Since LEFs are relative to a specified "terminal" distress level (D) and the associated number ( $N_t$ ) of axle applications, it is necessary to make these substitutions and to solve Equation 4 for  $N_t$  to yield:

$$N_t = (D/A_0)^{1/A_1} (L_1)^{-A_{21}/A_1} (L_2)^{-A_{22}/A_1} (S_1)^{-A_{31}/A_1} (S_2)^{-A_{32}/A_1} \dots (E_1)^{-A_{41}/A_1} (E_2)^{-A_{42}/A_1} \dots \quad \text{Equation 5}$$

By definition (Equation 1) the LEF for axle load X is the value of  $N_t$  for a standard axle load,  $N_t(S_2)$ , divided by  $N_t$  for the X axle load,  $N_t(XL)$ . Since  $L_1 = 18$  kips and  $L_2 = 1$  for the standard axle load, and the structural and environmental factors are the same, then the division produces the following relationship:

$$LEF(XL) = N_t(SL)/N_t(LX) = (18/L_{1x})^{-A_{21}/A_1} (1/L_{2x})^{-A_{22}/A_1}$$

or

$$LEF(XL) = (L_{1x}/18)^{B_1} / (L_{2x})^{B_2} \quad \text{Equation 6}$$

where  $B_1 = A_{21}/A_1$ ,  $B_2 = -A_{22}/A_1$ , and both are expected to be positive. Thus Equation 6 expresses LEF as a power function of the load ratio,  $L_{1x}/18$ , and is decreased by the configuration factor  $(L_{2x})^{B_2}$  when  $L_{2x}$  is greater than one. The load ratio power,  $B_1$ , is often called the load ratio exponent for LEF. If the value of  $B_1$  is 4, for example, then LEF is a fourth power function of the load ratio.

The logarithmic form of this equation is

$$\text{Log [LEF (XL)]} = B_1 \log (L_{1x}/18) - B_2 \log (L_{2x}) \quad \text{Equation 7}$$

and is basically a linear equation formulation which is a straight line when  $\log \text{LEF (XL)}$  is plotted against  $\log (L_{1x}/18)$ . In this formulation the ordinate (or Y) term is  $\log [\text{LEF(XL)}]$ , while the abscissa (or X) is  $\text{LOG}(L_{1x}/18)$ . The linear relationship defined as Equation 7 includes  $B_2 \log (L_{2x})$  as the constant and  $B_1$  as the slope. The origin (i.e.,  $y = 0 @ x = 0$ ) occurs when  $L_{1x} = 18$  and  $L_{2x} = 1$ , i.e., when the load ratio is  $L_{1x}/18 = 1$  and  $\text{LEF (XL)} = 1$  and consequently  $\log (L_{1x}/18)$ ,  $\log (L_{2x})$  and  $\log \text{LEF}$  are all zero.

It can be observed that the AASHO LEFs are very well approximated by Equations 6 or 7 with values for  $B_1$  and  $B_2$  as shown in Table 1.

From Table 1 it is obvious that  $B_1$  and  $B_2$  for the AASHO LEFs vary somewhat with pavement structure. Figures 1 and 2 show, respectively, the plots of Equation 7 for flexible pavements with a SN of 5 and for rigid pavements with a PCC thickness of 10". Table 1 indicates that slopes and intercepts of the lines in Figures 1 and 2 would generally be less for lesser structures, the exception being coefficient  $B_2$  for rigid pavement structures. (5)

For this study it has been established that LEFs and ESALs will be calculated from  $B_1$  and  $B_2$  values considered to be independent of structural and environmental factors. Thus, for given  $B_1$  and  $B_2$  values, a given traffic distribution will produce the same LEFs and ESALs for any structure - environment combination. Interactions between ESALs and structure or environment will be inferred from the results of regression analyses for the prediction of distress from ESALs, structural factors, and environmental factors.

## **AASHO Road Test PSI Relationships**

In the AASHO Road Test a Pavement Serviceability Rating Panel was assembled and instructed to assign, on a scale of 0 to 5, independent ratings of the ability of 138 sections of pavement, located in three states, to serve high speed, mixed truck and passenger traffic.

Both rigid and flexible pavements with anticipated ratings ranging from very poor to very good were included in the AASHO study. For each of the 138 sections the mean of the independent ratings of the panel members was considered to be the Section's Present Serviceability Rating or PSR (4).

A conventional multiple regression analysis procedure was used to correlate the Present Serviceability Ratings (PSRs) for the sections with actual measurements of longitudinal profile variations, cracking and patching for the rigid pavements, and cross profile variations, cracking and rutting for flexible pavements (4).

Table 1. Exponents for Approximation of AASHO LEFs by the Load Ratio Function

Axle Configuration	FLEXIBLE PAVEMENTS			RIGID PAVEMENTS		
	Structural Number	B <sub>1</sub>	B <sub>2</sub>	Thickness	B <sub>1</sub>	B <sub>2</sub>
Single	2	3.986	-	9	4.057	-
Single	4	3.858	-	11	4.122	-
Single	6	3.976	-	13	4.174	-
Tandem	2	3.897	3.089	9	4.003	2.73
Tandem	4	4.046	3.705	11	4.062	2.71
Tandem	6	4.206	3.918	13	4.115	2.69
Tridem	2	3.638	3.105	9	3.865	2.64
Tridem	4	3.786	3.367	11	3.924	2.64
Tridem	6	3.946	3.536	13	3.956	2.63

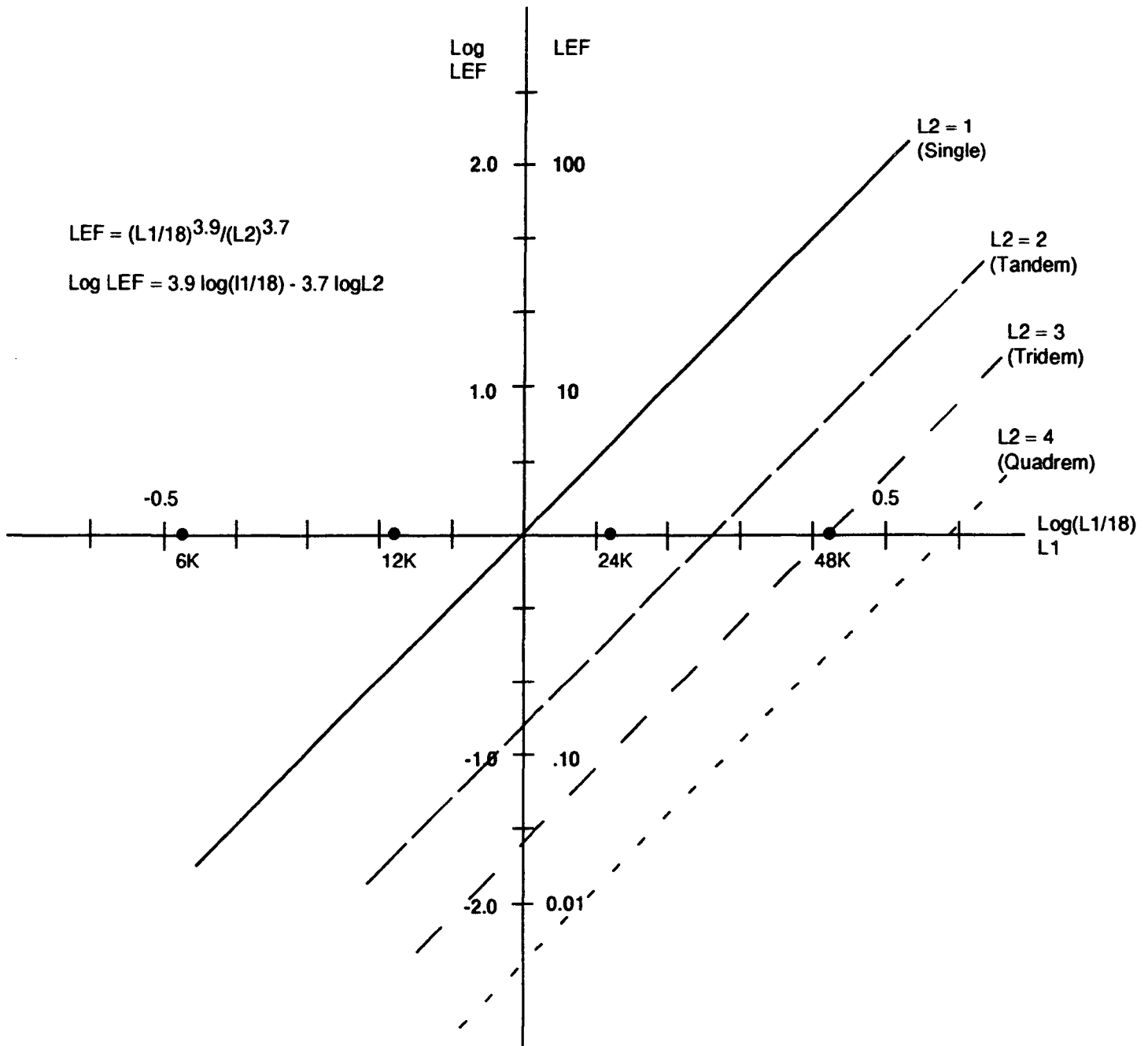


Figure 1. Power function approximations to AASHTO flexible pavement LEFs when SN = 5.

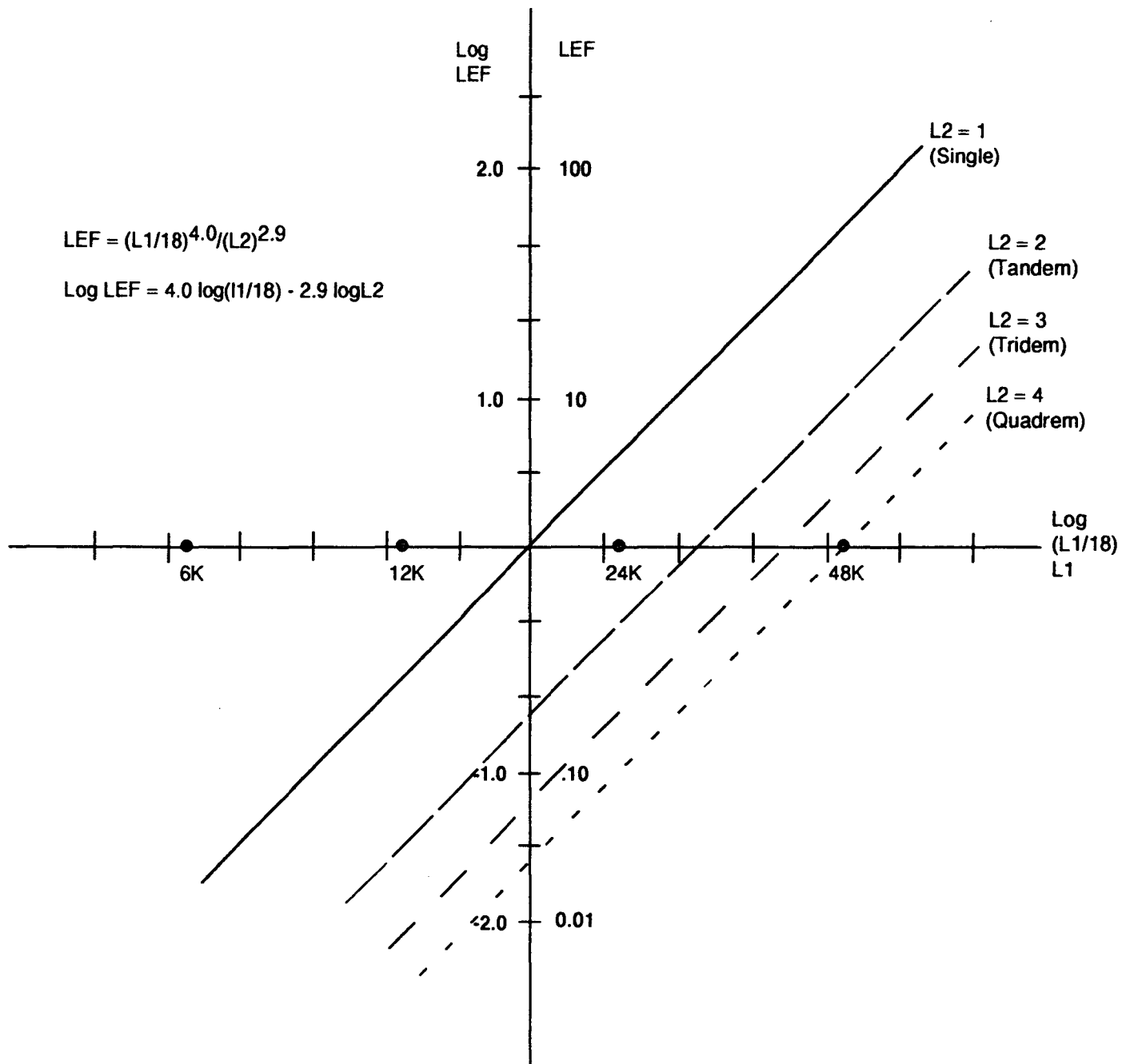


Figure 2. Power function approximation to AASHTO rigid pavement LEFs when PCC thickness = 10".

From this analysis, individual formulae were developed for rigid and flexible pavements which could be used to calculate a "Present Serviceability Index" closely approximating the mean (PSR) rating of the Panel (4). The PSI value is a numerical indicator of pavement performance and includes combinations of distress observations. The two PSI equations are presented below.

*Flexible Pavement (4)*

$$\text{PSI} = 5.03 - 1.91 \text{Log}_{10} (1+\overline{\text{SV}}) - .01 \sqrt{\text{C+P}} - 1.38 \text{RD}^2 \quad \text{Equation 8}$$

where

PSI = the present serviceability index

$\overline{\text{SV}}$  = the mean of the slope variance for the two wheelpaths

$\sqrt{\text{C+P}}$  = a measure of cracking and patching in the pavement surface

$\text{RD}^2$  = a measure of rutting in the wheelpaths

*Rigid Pavement (4)*

$$\text{PSI} = 5.41 - 1.80 \text{Log}_{10} (1+\overline{\text{SV}}) - .09 \sqrt{\text{C+P}} \quad \text{Equation 9}$$

where

PSI = the present serviceability index;

$\overline{\text{SV}}$  = the mean of the slope variance for the two wheelpaths; and

$\sqrt{\text{C+P}}$  = a measure of cracking and patching in the pavement surface

**SHRP-LTPP Approach to LEF Evaluation**

Since an LEF evaluation is a professed objective of the highway community for SHRP-LTPP, it seemed important that an initial study be undertaken to develop a plan and/or approach for just such an investigation. Although there are a number of pavement distress manifestations which could be investigated in a study of this type, it seems logical to limit the distresses to a smaller number of classical representations so that the proposed approach and results can be evaluated with a reasonable work effort.

In the pursuit of the SHRP-LTPP LEF study (9), it was recognized that present serviceability estimates (10), serviceability loss (11), and traffic estimates (12) would all be needed to accomplish the proposed evaluation. The results of these work efforts were important elements in an evaluation of the LEF approach (9) proposed for this study (6). The evaluation included both rigid and flexible pavement sections (see Table 2).

Since a single summary index such as PSI cannot distinguish between combinations of distress to meet various maintenance and rehabilitation trigger levels (4) it is proposed that the SHRP-LTPP LEF study include separate investigations of roughness, rutting, and cracking (fatigue) for the flexible pavement sections and roughness and cracking (fatigue) for the rigid pavements. These selections are based on the distress manifestations (i.e., roughness, cracking, rutting) defined in the original AASHO PSI equation (Equations 8 and 9).

## LEF Evaluation Techniques

Conventional multiple regression analysis techniques were used to generate individual distress prediction equations for roughness, rutting and serviceability loss in the case of flexible pavements and for roughness and serviceability loss in the case of rigid pavements. It was originally proposed that the evaluation include cracking in both the flexible and rigid pavements, however, the paucity of distress data in the SHRP-LTPP database eliminated this option.

For a particular LTPP section a series of regression equations using various combinations of  $B_1$  and  $B_2$  exponents were developed that relate pavement performance (e.g., rutting, roughness, PSI loss) to cumulative ESALs, annual ESALs, and pavement structural and site environmental conditions. Each regression analysis has a coefficient of determination ( $R^2$ ), a standard error of estimate (RMSE), and a coefficient of variation (CV). These statistics quantify the goodness of fit of the particular predictive equation. It is expected that comparisons of these statistics, along with consideration of the regression coefficients and their standard errors, will indicate which combinations of  $B_1$  and  $B_2$  values lead to "best" fits.

Interaction effects (represented by cross-product terms of ESALs, pavement structure, and environment) are expected to be important indicators of the extent to which ESAL effects vary with structural and environmental factors.

## Rigid Pavement LEF Evaluation

The pavement performance indicators evaluated in this study include roughness and PSI loss. The roughness indicator is the IRI generated by the SHRP Law profilometers. PSI-Loss was defined as the difference between an assumed initial PSI value of about 4.5 (similar to AASHO Road Test Analysis (4) and a present serviceability value. The present serviceability value was developed from the following equation using the profilometer-generated IRI value.

$$PSI = 6.52 - 1.79 \log(IRI) \quad (10)$$

Equation 10

Table 2 Flexible and Rigid Pavement Sections Included in the LEF Study

Section	State	Pavement Type
062051	California	Flexible
062647	California	Flexible
068201	California	Flexible
182008	Indiana	Flexible
382001	North Dakota	Flexible
512004	Virginia	Flexible
063042	California	Rigid
124000	Florida	Rigid
183031	Indiana	Rigid
385002	North Dakota	Rigid
485336	Texas	Rigid
537409	Washington	Rigid

The structural and environmental factors included in an evaluation of the proposed LEF approach to rigid pavement analysis are presented in Table 3. The performance data including IRI, PSI, and PSI-Loss are also included in the table. The cumulative ESALs for each pavement section at each combination of  $B_1$  and  $B_2$  are presented in Table 4.

### *Evaluation of log(IRI)*

The equation for roughness, measured as IRI, for the rigid pavement sections is a logarithmic form including cross-products of log(Annual ESALs) and log of moisture and temperature. The form is as follows:

$$\begin{aligned} \log(\text{IRI}) = & K_1 + K_2 * [\log(\text{ESALs}) * \log(\text{MOIST})] \\ & + K_3 * [\log(\text{ESALs}) * \log(\text{TEMP})] \end{aligned} \quad \text{Equation 11}$$

where

MOIST = Moisture conditions: dry +1, wet +2  
TEMP = Temperature zone: nonfreeze +1, freeze +2  
 $K_1, K_2, K_3$  = regression coefficients

The regression analysis results are presented in Table 5.

The combination of  $B_1 = 4.0$  and  $B_2 = 3.0$  represents the normal AASHO-type LEF coefficients. In this analysis, however, the combination of  $B_1 = 3.0$  and  $B_2 = 3.5$  produced the highest  $R^2$  value, the lowest RMSE, and the lowest CV. This combination apparently fulfills the best fit criteria and can be considered in possible development of new LEFs.

### *Evaluation of log(PSI-Loss)*

The equation for AASHO PSI-Loss (4.2 - present serviceability,  $p$ ) for rigid pavement sections is a logarithmic form including cross products of log(Cumulative ESALs) and log of moisture and log of temperature. The form of the equation is

$$\begin{aligned} \log(\text{PSI-Loss}) = & K_1 + K_2 \{ \log(\text{Cumulative ESALs}) * \log(\text{MOIST}) \} \\ & + K_3 \{ \log(\text{Cumulative ESALs}) * \log(\text{TEMP}) \} \end{aligned} \quad \text{Equation 12}$$

Table 3 Structural and Environmental Factors - Rigid Pavement Sections

Section	Modulus, PSI	Poisson's Ratio	Modulus of Subgrade Reaction PSI	Thickness Inches	Moisture Zone	Temp. Zone	Subgrade Type	Age Yrs.	IRI	PSI	PSI- Loss
063042	3,475,000	.130	696	8.83	D	NF	F	12.0	60.49	3.33	1.17
124000	3,575,000	.145	535	8.08	W	NF	C	17.0	104.32	2.91	1.59
183031	4,875,000	.220	289	10.20	W	F	F	15.0	98.50	2.95	1.55
385002	5,000,000	.180	-	8.00	D	F	F	18.0	81.00	3.10	1.40
485336	4,425,000	.110	-	8.90	D	NF	F	4.0	50.00	3.48	1.20
537409	3,425,000	.175	629	9.33	D	F	C	3.0	76.44	3.15	1.35

Table 4 Estimates for Rigid Sections

Section	B <sub>1</sub>	B <sub>2</sub>	Cumulative ESALS
063042	2.0	2.0	14355454
	2.0	5.0	9305129
	3.0	3.0	11456752
	3.0	3.5	10027178
	4.0	3.0	14272518
	4.0	3.5	11727072
	5.0	2.0	37044044
	5.0	5.0	9093695
124000	2.0	2.0	1852575
	2.0	5.0	1286152
	3.0	3.0	1553494
	3.0	3.5	1362074
	4.0	3.0	2244204
	4.0	3.5	1793670
	5.0	2.0	9009065
	5.0	5.0	1581034
183031	2.0	2.0	1832217
	2.0	5.0	933100
	3.0	3.0	1351484
	3.0	3.5	1096509
	4.0	3.0	1955054
	4.0	3.5	1481141
	5.0	2.0	6671511
	5.0	5.0	1070818
485336	2.0	2.0	1538856
	2.0	5.0	731892
	3.0	3.0	1114260
	3.0	3.5	901940
	4.0	3.0	1499312
	4.0	3.5	1139418
	5.0	2.0	4583394
	5.0	5.0	752490
537409	2.0	2.0	1339331
	2.0	5.0	706154
	3.0	3.0	1157885
	3.0	3.5	9660258
	4.0	3.0	1779917
	4.0	3.5	1390438
	5.0	2.0	6529325
	5.0	5.0	1190595

Table 4 Estimates for Rigid Sections (Continued)

Section	B <sub>1</sub>	B <sub>2</sub>	Cumulative ESALS
385002	2.0	2.0	1243383
	2.0	5.0	659016
	3.0	3.0	751133
	3.0	3.5	609317
	4.0	3.0	904717
	4.0	3.5	684333
	5.0	2.0	2572366
	5.0	5.0	406800

Table 5 Regression Analysis Results, log(IRI), for Rigid Pavement Analysis

$B_1$	$B_2$	$R^2$	RMSE	CV	$K_1$	$K_2$	$K_3$
2.0	2.0	.8009	.0706	3.75	1.77140	.0988	.0508
2.0	5.0	.8078	.0694	3.69	1.77031	.1031	.0541
3.0	3.0	.8024	.0703	3.74	1.77118	.1006	.0521
3.0	3.5	.8092	.0691	3.68	1.76925	.1041	.0506
4.0	3.0	.8012	.0705	3.75	1.77142	.0980	.0507
4.0	3.5	.8023	.0703	3.74	1.77124	.0998	.0518
5.0	2.0	.8033	.0702	3.73	1.77110	.0901	.0470
5.0	5.0	.8051	.0698	3.71	1.77982	.1017	.0533

$$\log(\text{IRI}) = K_1 + K_2 * [\log(\text{ESALs}) * \log(\text{MOIST})] + K_3 [\log(\text{ESALs}) * \log(\text{TEMP})]$$

where

MOIST = Moisture conditions: dry +1, wet +2  
TEMP = Temperature conditions: nonfreeze +1, freeze +2  
 $K_1, K_2, K_3$  = regression coefficients

The regression analysis results are presented in Table 6.

In this instance the combination of  $B_1 = 3.0$  and  $B_2 = 3.5$  again produced the best fit for Equation 12, although all other combinations yielded similar characteristics. The 3, 3.5 combination yielded the highest  $R^2$ , and the lowest RMSE but the CV for the equation is high, at about 34%.

### **Regional Aspects of Rigid Pavement Performance**

The equations for  $\log(\text{IRI})$  and  $\log(\text{AASHO PSI-Loss})$  can be further compartmentalized into environmental zones considering moisture (i.e., dry versus wet) and temperature (i.e., nonfreeze versus freeze) combinations. Using this approach, equations have been generated for the four environmental zones to predict pavement roughness (see Table 7) and serviceability trends (see Table 8) for the rigid pavements included in this study.

For each performance variable it can be seen from Tables 7 and 8 that the impact of traffic varies from environmental zone to environmental zone. The dry nonfreeze zones apparently experience less destructive effects due to traffic loading (or cumulative ESALs) and the greatest destructive effects are produced by traffic loadings (or cumulative ESALs) in the wet-freeze environment zone.

### *Possible Effects on LEF values for Rigid Pavements*

A comparison of the LEF values of the best fit combination (3.0, 3.5) with the AASHO combination (4.0, 3.0) leads to the conclusion that the acceptance of the use of the combination of  $B_1 = 3.0$  and  $B_2 = 3.5$  could result in the following changes in AASHO-type (IRI) and  $\log(\text{PSI-Loss})$ :

#### Increase in LEFs

Single Axles below 18 kips  
Tandem Axles below 12 kips

#### Decrease in LEFs

Single Axles above 18 kips  
Tandem Axles above 12 kips  
Tridem Axles (all loads)  
Quadrem Axles (all loads)

Table 6 Regression Analysis Results, log(4.2-PSI) for Rigid Pavement Analysis

$B_1$	$B_2$	$R^2$	RMSE	CV	$K_1$	$K_2$	$K_3$
2.0	2.0	.7756	.04444	34.0	.06531	.05587	.03255
2.0	5.0	.7824	.04376	33.5	.06467	.05831	.03459
3.0	3.0	.7770	.04430	33.9	.06518	.05692	.03337
3.0	3.5	.7846	.04354	33.3	.06396	.05904	.03242
4.0	3.0	.7757	.04444	34.0	.06532	.05541	.03249
4.0	3.5	.7766	.04433	33.9	.06522	.05645	.03318
5.0	2.0	.7777	.04423	33.9	.06514	.05095	.03008
5.0	5.0	.7794	.04406	33.7	.06499	.05753	.03414

$$\log(\text{PSI-Loss}) = K_1 + K_2 * [\log(\Sigma\text{ESALs}) * \log(\text{MOIST})] + K_3 [\log(\Sigma\text{ESALs}) * \log(\text{TEMP})]$$

Table 7 log(IRI) for PCC Jointed Pavements

<p><i>Basic Equation</i></p> $\log(\text{IRI}) = 1.76925 + 0.104103 [\log(\Sigma\text{ESALs}) * \log(\text{MOIST})] + 0.05069 * [\log(\Sigma\text{ESALs}) * \log(\text{TEMP})]$
<p><i>Dry-Nonfreeze Zone (M = +1, T = +1)</i></p> $\log(\text{IRI}) = 1.76925$ $\text{IRI} = 58.78$
<p><i>Dry-Freeze Zone (M = +1, T = +2)</i></p> $\log(\text{IRI}) = 1.76025 + 0.01526 \log(\Sigma\text{ESALs})$ $\text{IRI} = 58.78 (\Sigma\text{ESALs})^{0.01526}$
<p><i>Wet-Nonfreeze Zone (M = +2, T = +1)</i></p> $\log(\text{IRI}) = 1.76925 + 0.03134 \log(\Sigma\text{ESALs})$ $\text{IRI} = 58.78 (\Sigma\text{ESALs})^{0.03134}$
<p><i>Wet-Freeze Zone (M = +2, T = +2)</i></p> $\log(\text{IRI}) = 1.76925 + 0.04660 \log(\Sigma\text{ESALs})$ $\text{IRI} = 58.78 (\Sigma\text{ESALs})^{0.04660}$

Table 8 log(4.2 - PSI) for PCC Jointed Pavements

<p><i>Basic Equation</i></p> $\log(\text{PSI-4.2}) = .06396 + 0.05904 [\log(\Sigma\text{ESALs}) * \log(\text{MOIST})] + .03242 * [\log(\Sigma\text{ESALs}) * \log(\text{TEMP})]$
<p><i>Dry-Nonfreeze Zone (M = +1, T = +1)</i></p> $\begin{aligned} \text{Log(4.2-PSI)} &= + 0.06396 \\ (4.2\text{-PSI}) &= 1.159 (\Sigma\text{ESALs})^0 \end{aligned}$
<p><i>Dry-Freeze Zone (M = +1, T = +2)</i></p> $\begin{aligned} \log(4.2\text{-PSI}) &= 0.06396 + 0.00976 \log(\Sigma\text{ESALs}) \\ (4.2\text{-PSI}) &= 1.159 (\Sigma\text{ESALs})^{.00976} \end{aligned}$
<p><i>Wet-Nonfreeze Zone (M = +2, T = +1)</i></p> $\begin{aligned} \log(4.2\text{-PSI}) &= 0.06396 + 0.01777 \log(\Sigma\text{ESALs}) \\ (4.2\text{-PSI}) &= 1.159 (\Sigma\text{ESALs})^{0.01777} \end{aligned}$
<p><i>Wet-Freeze Zone (M = +2, T = +2)</i></p> $\begin{aligned} \log(4.2\text{-PSI}) &= 0.06396 + 0.02753 \log(\Sigma\text{ESALs}) \\ (4.2\text{-PSI}) &= 1.159 (\Sigma\text{ESALs})^{0.02753} \end{aligned}$

## Flexible Pavement LEF Evaluation

The pavement performance indicators evaluated in this study included rutting, roughness, and PSI-Loss. The rutting indicator is defined with a classical AASHO definition in units of millimeters, while the roughness is characterized by the IRI values generated by the SHRP-LTPP Law profilometer. PSI-Loss is defined in two ways. The first involves a value defined as the difference between an initial estimate of 4.2 (similar to that assumed in the AASHO Road Test equation) and the present serviceability level. It should be noted that this approach negates the influence of variation in initial serviceability estimates, since a fixed value of 4.2 is defined for all sections. The second method involves the use of the PSI-Loss estimates obtained from the following equations that was developed as a part of this study:

$$\text{SHRP PSI Loss} = \left[ \frac{K}{1-K} \right] * (p_n - 2.0) \quad (11) \quad \text{Equation 13}$$

where

$p_n$  = present serviceability at time  $n$ ,  
 $K$  is defined by the following equations:

$$K = 0.6718 + 0.156 * (\text{TEMP}) + 2.605 \times 10^{-6} * (\text{ESALs}) + 0.0625 * (\text{SUBG} * \text{MOIST}) - 0.8306 \times 10^{-6} * (\text{ESALs} * \text{SN}) \quad \text{Equation 14}$$

where

TEMP = temperature zone: nonfreeze -1, freeze +1

ESALs = annual ESALs rate or  $\sum_0^n \text{ESALs}/n$  years

SUBG = subgrade type: fine-grained +1, coarse-grained +2

MOIST = moisture conditions: dry -1, wet +1

SN = structural number of the pavement section

The present serviceability value was estimated from the following equation using the profilometer-generated IRI value:

$$\text{PSI} = 6.52 - 1.79 \log(\text{IRI}) \quad (10)$$

The structural and environmental factors included in an evaluation of the proposed LEF approach for flexible pavements are presented in Table 9. The performance data including rutting, IRI, PSI-4.2 and PSI-Loss are also included in the table.

Table 9 Environmental and Structural Information for Flexible Pavement Sections

Section ID	Structural Number	Asphalt Content	Asphalt Density	Air Voids	Sub-grade	Moisture Zone	Temp. Zone	Surface Thickness in.	Base Thickness in.	Esg, ksi
062051	3.78	4.9	144.6	7.3	-1	-1	-1	5.0	6.5	40.65
062647	3.68	5.0	150.3	2.3	-1	-1	-1	3.7	5.3	31.98
068210	3.50	5.3	134.5	11.1	-1	-1	-1	4.5	4.8	33.55
182008	7.15	4.6	147.0	6.9	+1	+1	+1	2.6	5.4	22.02
382001	2.88	6.3	145.6	2.9	-1	-1	+1	2.4	6.3	13.51
512004	4.70	5.5	133.0	1.9	-1	+1	+1	1.5	7.0	21.17

Section ID	Eb ksi	Es, ksi	Freeze Index Days	Annual Precipitation (in.)	Days Over 90%	Rut Depth, (mm)	IRI	PSI
062051	97.51	683.05	1	26.51	22	4.78	105.22	2.87
062647	175.92	869.32	2	27.05	74	4.24	87.85	3.01
068210	710.16	867.07	0.2	8.80	113	2.66	57.83	3.34
182008	220.78	530.95	773	37.51	12	10.63	142.32	2.65
382001	40.81	768.26	2623	19.35	8	8.14	120.03	2.77
512004	119.60	847.46	121	44.70	48	3.83	85.73	3.15

LEGEND

Es = modulus of surface layer  
 Eb = modulus of base layer  
 Esg = modulus of subgrade

The cumulative ESALs for each pavement section at each combination of coefficients,  $B_1$  and  $B_2$ , are presented in Table 10.

### *Evaluation of Rutting*

The equation for rutting (in millimeters) in the flexible pavement sections is a logarithmic form including a main effect of  $\log(\text{Cumulative ESALs})$  and a cross-product containing  $\log(\text{Surface Layer Modulus})$  and  $\log(\text{Cumulative ESALs})$ . The form of the equation is:

$$\log(\text{RUT}) = K_1 + K_2 * \log(\Sigma\text{ESALs}) + K_3 [\log(E_{\text{SURF}}) * \log(\Sigma\text{ESALs})] \quad \text{Equation 15}$$

where

$\Sigma\text{ESALs}$  = cumulative ESALs based on  $B_1$  and  $B_2$  values

$E_{\text{SURF}}$  = surface layer modulus in ksi

$K_1, K_2, K_3$  = regression coefficients

The regression analysis results are presented in Table 11. In this instance the combination of  $B_1 = 5.0$  and  $B_2 = 2.0$  produces the equation with the highest  $R^2$  value, lowest RMSE, and lowest CV for Equation 15. The AASHTO combination of  $B_1$  and  $B_2$  yielded the next best combination of regression equation attributes (i.e.,  $R^2$ , RMSE, and CV). It should be noted that a  $B_1$  coefficient of 5.0 is relatively high and could indicate the principal influence and magnitude of wheel load on the development of rutting.

### *Evaluation of Roughness (IRI)*

The equation for roughness is also based on a logarithmic form, including a main effect of  $\log(\text{Cumulative ESALs})$  and a cross-product of  $\log(\text{Cumulative ESALs})$  and  $\log(\text{Surface Layer Modulus})$ . The form of the equation is:

$$\log(\text{IRI}) = K_1 + K_2 * \log(\Sigma\text{ESALs}) + K_3 * [\log(E_{\text{SURF}}) * \log(\Sigma\text{ESALs})] \quad \text{Equation 16}$$

where

$\Sigma\text{ESALs}$  = cumulative ESALs based on  $B_1$  and  $B_2$  values

$E_{\text{SURF}}$  = surface layer modulus in ksi

$K_1, K_2, K_3$  = regression coefficients

The regression analysis results are presented in Table 12. In a review of the regression analysis results, there were four combinations of  $B_1$  and  $B_2$  values that yielded high  $R^2$  values; however, the AASHTO combination produced the equation with the highest  $R^2$  (0.9547), lowest RMSE (0.0374), and lowest CV (1.89) for Equation 16. Therefore, in the case of longitudinal roughness in flexible pavements, the AASHTO LEFs apparently produce cumulative ESAL

Table 10 Traffic Estimates for Flexible Sections

Section	B <sub>1</sub>	B <sub>2</sub>	Cumulative ESALS
062051	2.0	2.0	957042
	3.0	3.0	650683
	3.0	3.5	584381
	4.0	3.0	615510
	4.0	3.5	533475
	5.0	2.0	1139103
	5.0	5.0	385083
062647	2.0	2.0	136273
	3.0	3.0	93984
	3.0	3.5	88672
	4.0	3.0	85227
	4.0	3.5	77162
	5.0	2.0	139980
	5.0	5.0	59138
068201	2.0	2.0	104158
	3.0	3.0	68476
	3.0	3.5	64296
	4.0	3.0	67545
	4.0	3.5	59812
	5.0	2.0	143526
	5.0	5.0	49571
182008	2.0	2.0	4340679
	3.0	3.0	3483753
	3.0	3.5	2814283
	4.0	3.0	5208966
	4.0	3.5	3957471
	5.0	2.0	17625164
	5.0	5.0	2907597
382001	2.0	2.0	403580
	3.0	3.0	316230
	3.0	3.5	244210
	4.0	3.0	493120
	4.0	3.5	360870
	5.0	2.0	1716820
	5.0	5.0	236890

Table 10 Traffic Estimates for Flexible Sections (Continued)

Section	B <sub>1</sub>	B <sub>2</sub>	Cumulative ESALS
512004	2.0	2.0	4583380
	3.0	3.0	3944001
	3.0	3.5	3251052
	4.0	3.0	6180206
	4.0	3.5	4766663
	5.0	2.0	22168583
	5.0	5.0	3896169

Table 11 Regression Analysis Results, log(RUT), Flexible Pavement Analysis

$B_1$	$B_2$	$R^2$	RMSE	CV	$K_1$	$K_2$	$K_3$
2.0	2.0	0.8619	0.10630	15.00	-2.38762	-0.10389	0.30650
3.0	3.0	0.9041	0.00861	12.50	-2.23987	-0.14769	0.24186
3.0	3.5	0.8559	0.10861	15.30	-2.27780	-0.14214	0.24438
4.0	3.0	0.9801	0.04036	5.70	-2.00502	-0.08074	0.10358
4.0	3.5	0.9612	0.05633	7.93	-2.0930	-0.18720	0.24719
5.0	2.0	0.9882	0.03102	4.38	-1.74810	-0.18691	0.21268
5.0	5.0	0.9405	0.06979	9.85	-2.16001	-0.22120	0.26801
AASHTO		0.9872	0.0323	4.56	-2.12273	-0.16791	0.24205

$$\log(\text{RUT}) = K_1 + K_2 * \log(\Sigma\text{ESALs}) + K_3 * [\log(E_{\text{SURF}} * \log(\Sigma\text{ESALs}))]$$

Table 12 Regression Analysis Results - AASHO Serviceability Loss  
Flexible Pavement Analysis

$B_1$	$B_2$	$R^2$	RMSE	CV	$K_1$	$K_2$	$K_3$
2.0	2.0	0.0959	0.0200	5.76	-0.3736	-0.0307	0.0561
3.0	3.0	0.9220	0.0182	5.25	-0.3287	-0.0405	0.0578
3.0	3.5	0.8991	0.0207	5.97	-0.3460	-0.0408	0.0595
4.0	3.0	0.9184	0.0186	5.37	-0.2488	-0.0206	0.0238
4.0	3.5	0.9209	0.0103	5.29	-0.2751	-0.0483	0.0573
5.0	2.0	0.8391	0.0261	7.54	-0.1660	-0.0453	0.0467
5.0	5.0	0.8913	0.0215	6.19	-0.2864	-0.0557	0.0616
AASHTO		0.9388	0.0161	4.65	-0.2794	-0.0438	0.0559

$$\log(1 + \text{AASHO PSI-Loss}) = K_1 + K_2 * \log(\Sigma\text{ESALs}) + K_3 * [\log(\Sigma\text{ESALs}) * \log(E_{\text{SURF}})]$$

estimates that correspond to the level of roughness developed in the flexible pavement sections included in this study.

### *Evaluation of AASHO Serviceability Loss*

The equation for AASHO serviceability loss is a logarithmic form including

$$\log[1 + (4.2 - p)] = K_1 + K_2 * \log(\Sigma\text{ESALs}) + K_3 [\log(\Sigma\text{ESALs}) * \log(E_{\text{SURF}})] \quad \text{Equation 17}$$

where

- 4.2 - p = AASHO Serviceability Loss
- ΣESALs = cumulative ESALs based on B<sub>1</sub> and B<sub>2</sub> values
- E<sub>SURF</sub> = surface layer modulus in ksi
- K<sub>1</sub>, K<sub>2</sub>, K<sub>3</sub> = regression coefficients

From this portion of the study it was found that the best fit equation for log(1 + AASHO Serviceability Loss) corresponds to the B<sub>1</sub> and B<sub>2</sub> combinations identified with the original AASHO LEFs. Although (B<sub>1</sub>, B<sub>2</sub>) combinations (3.0, 3.0 and 4.0, 3.5) yielded acceptable regression equation attributes, the AASHO-based combination yielded the equation with the highest R<sup>2</sup>, lowest RMSE, and lowest CV for Equation 17.

Based on these results, the AASHO LEF values will apparently yield cumulative ESAL estimates that correspond well to pavement serviceability trends. This is not unexpected, since the original AASHO road test serviceability concept is based on a serviceability loss factor established for an initial PSI value of 4.2.

### *Evaluation of SHRP Serviceability Loss $[\{K/(1-K)\}(p_n-2.0)]$*

The SHRP serviceability loss estimate for this investigation was generated from an equation for K [or (W/p)<sup>β</sup>] that was developed from the results of six different road test evaluations, including Loop 4 of the AASHO Road Test (4).

where

- W = cumulative 18 KESALs applied at end of time, t
- p = function of design and load variables denoting the expected number of axle load applications to a terminal serviceability
- β = a function of design and load variables that influence the shape of serviceability (p), versus cumulative ESALs (W), curve

The equation for  $K$  is

$$K = (W/p)^b = 0.06718 * 0.1560 * (\text{TEMP}) + 2.605 * 10^{-6} * (\text{ESALs}) + 0.0625 * (\text{SUBG} * \text{MOIST}) - 0.8306 * 10^{-6} * (\text{ESALs} * \text{SN}) \quad \text{Equation 18}$$

where

- TEMP = temperature zone: nonfreeze -1, freeze +1
- ESALs = annual average ESAL rate or  $(\sum_0^n \text{ESALs}/n)$
- SUBG = subgrade type: fine-grained +1, coarse-grained +2
- MOIST = moisture conditions: dry -1, wet +1
- SN = structural number of the pavement section

The equation for the SHRP-estimated serviceability loss for flexible pavement sections is a logarithmic form including cross-products of log(Subgrade Modulus) by log(Cumulative ESALs) and log(Precipitation) by log(Days over 90°F). The form of the equation is as follows:

$$\log(\text{SHRP PSI Loss}) = K_1 + K_2 * [\log(\text{Esg}) * \log(\sum \text{ESALs})] + K_3 * [\log(\text{PRECIP}) * \log(\text{Days})] \quad \text{Equation 19}$$

where

- SHRP PSI Loss =  $[K/K-1] * (p_n - 2.0)$
- $p_n$  = present serviceability index
- Esg = subgrade modulus in ksi
- $\sum \text{ESALs}$  = cumulative ESALs for combination of  $B_1$  and  $B_2$  values
- PRECIP = annual precipitation in inches/year
- DAYS = average annual number of days over 90°F
- $K_1, K_2, K_3$  = regression coefficients

The regression analysis results are presented in Table 13. Three combinations of  $B_1$  and  $B_2$  [i.e., (2, 2), (3, 3), (3, 3.5)] produced equations with better attributes than the AASHO combination of  $B_1$  and  $B_2$ . Of the four combinations, however, the best fit was obtained for the combination of  $B_1 = 3$  and  $B_2 = 3.5$ . The equation has the highest  $R^2$ , the lowest RMSE, and the lowest CV.

From a general assessment of the equation, it can be inferred that serviceability loss is reduced for higher subgrade moduli, higher precipitation rates, and higher number of days exceeding 90°F.

Table 13. Regression Analysis Results - SHRP Serviceability Loss  
Flexible Pavement Analysis

$B_1$	$B_2$	$R^2$	RMSE	CV	$K_1$	$K_2$	$K_3$
2.0	2.0	0.8735	0.0595	19.49	1.303	-0.0848	-0.0651
3.0	3.0	0.8548	0.0637	20.88	1.1098	-0.0838	-0.0067
3.0	3.5	0.8621	0.0621	20.35	1.1040	-0.0846	-0.0644
4.0	3.0	0.8123	0.0724	23.74	1.0913	-0.0340	-0.0755
4.0	3.5	0.8247	0.0700	22.95	1.0921	-0.0804	-0.0718
5.0	2.0	0.7646	0.0811	26.59	1.0787	-0.0695	-0.0852
AASHTO		0.8137	0.0722	23.66	1.1121	-0.0823	-0.0745

$$\log(1+\delta\text{PSI}) = K_1 + K_2 * \log(\text{Esg}) * \log(\Sigma\text{ESALs}) + K_3 * \log(\text{Precipitation}) \\ * \log(\text{Days over } 90^\circ\text{F})$$

## Possible Effect on LEF Values for Flexible Pavements

A comparison of the best fit combinations of  $B_1$  and  $B_2$  for the four performance variables leads to the possibility that the acceptance of best fit values could result in the LEF changes identified in Table 14. No changes are expected in AASHTO LEFs for IRI and AASHTO PSI-Loss. On the other hand, the AASHTO LEFs could be significantly increased for all axle configurations if pavement rutting is predicted. In the case of the SHRP serviceability loss, the LEFs could be increased for loads below 18,000 pounds and decreased for loads exceeding 18,000 pounds.

## *Conclusions and Recommendations*

The results of this study indicate that the approach proposed for improving AASHTO LEFs using SHRP-LTPP data is viable. In addition, it appears that the data contained in the SHRP-LTPP database are sufficient to conduct a comprehensive study. It is recommended that an expanded analysis be undertaken in the near future when additional performance and traffic data are available.

Table 14 Possible LEF Changes Identified in This Study

Performance Variable	Load Level (thousands of pounds)	Impact on LEFs by Axle Type			
		Single	Tandem	Tride	Quadrem
<b>Rutting</b>					
B <sub>1</sub> = 5.0	<18	Smaller	Greater	Greater	Greater
B <sub>2</sub> = 2.0	>18	Greater	Greater	Greater	Greater
<b>IRI</b>					
B <sub>1</sub> = 3.9	<18	Same	Same	Same	Same
B <sub>2</sub> = 3.5	>18	Same	Same	Same	Same
<b>AASHO PSI-Loss</b>					
B <sub>1</sub> = 3.9	<18	Same	Same	Same	Same
B <sub>2</sub> = 3.5	>18	Same	Same	Same	Same
<b>SHRP PSI-Loss</b>					
B <sub>1</sub> = 3.0	<18	Greater	Greater	Greater	Not Available
B <sub>2</sub> = 3.5	>18	Smaller	Smaller	Smaller	Smaller

# Materials and Construction Variability Study

One of the objectives of SHRP-LTPP was to investigate the effects of materials properties, materials variability, and construction quality on pavement performance (2). The goal was to find a way to incorporate these variables into specific predictive equations for rigid and flexible pavement performance parameters.

## Approach

In this study the construction variability factors were classified as Distress and Performance Variables, Primary Structural Factors, Materials Properties, and Nonstructural Variables (see Figure 3). Consequently, the conceptual distress prediction model is composed of a nonstructural variables component (traffic, environment, age, etc.), a structural and materials factor means component, and a third component involving structural and materials factor variances (see Figure 4).

The actual analytical approach used in this investigation (6) consisted of a linear regression analysis relating the log of a pavement performance or distress variable to the logs of the nonstructural variables, logs of mean structural and materials factors, logs of variances of structural and materials factors, and their cross-products (Figure 5). The factors composing the regression equations can then be used to identify the factors and/or variances that significantly effect the specific pavement performance or distress variable.

## Construction Variability in Rigid Pavements

The construction variability factors included in the rigid pavement investigation are identified below. The specific site information and data for the LTPP sections investigated in the rigid pavement construction variability study are presented in Table 15.

### *Rigid Pavement Construction Variability Factors*

#### Distress and Performance Variables (*D*)

International Roughness Index (IRI)

AASHO PSI-Loss

#### Primary Structural Variables (*S*)

Portland Cement Concrete (PCC) Layer Thickness

PCC Layer Modulus

PCC Layer Poisson's Ratio

Modulus of Subgrade Reaction (*K*)

### Distress and Performance Variables (*D*)

- Rutting
- Roughness
- Present Serviceability Index (PSI)
- Cracking

### Primary Structural Factors (*S*)

- Layer Thicknesses
- Layer Moduli
- Subgrade Moduli

### Materials Properties (*M*)

- Mix Design Variables
- Layer Properties

### Nonstructural Variables (*E*)

- Traffic (KESALs)
- Environment
- Moisture

**Figure 3 Construction Variability Factors**

D, distress function, is a function of

f (ESALs; Environment)

\*

g (Structural Factor Means  $S_1, S_2$ , etc.;

Materials Factor Means  $M_1, M_2$ , etc.)

\*

h (Structural Factor Variances  $S_1^2, S_2^2$ , etc.;

Materials Factor Variances  $M_1^2, M_2^2$ , etc.)

Figure 4. Distress Prediction Model

- Linear Regression Using logarithms:

$\log D$

$\log \text{KESALs}$

$\log S_1$

•

•

$\log M_1$

•

•

$\log (S_1^2)$

•

•

$\log (M_1^2)$

- Significant Effects

Figure 5. Actual Analytical Approach

Table 15. Site Specific Information and Data -  
Rigid Pavement Construction Variability Study.

SHRP Section	Traffic (KESAL)	PCC Modulus (PSI)	PCC Modulus (Std Dev)	PCC Poisson's Ratio	PCC Poisson's Ratio (Std Dev)	Modulus of Subgrade Reaction (PCI)	Modulus of Subgrade Reaction (Std Dev)
47614	18533.0	4449998	636396	0.115	0.021	435.25	66.27
63010	3137.0	3550002	424264	0.200	---	1029.92	247.87
63013	2699.0	4175000	388909	0.150	0.042	403.37	150.87
63017	1631.0	4100001	282843	0.195	0.007	468.15	95.04
63042	14557.0	3474998	35355	0.130	---	695.95	150.84
123811	798.0	3050002	70711	0.165	0.007	1881.99	380.10
124000	4312.0	3575000	106066	0.145	0.007	534.83	120.91
133015	1076.0	4124997	176777	0.115	0.007	587.25	223.14
133017	2372.0	3449999	282843	0.145	0.021	543.55	92.53
133018	3356.0	4723998	---	0.150	---	394.74	220.57
163017	3296.0	4550000	141421	0.170	0.014	677.05	167.40
183031	5714.0	4874998	176777	0.220	0.014	289.12	56.80
203015	813.0	4199998	1202081	0.270	0.028	288.52	24.47
233013	3653.0	4550000	919239	0.185	0.049	189.20	62.64
233014	3203.0	3374999	247487	0.175	0.021	370.61	31.65
313028	645.0	4924999	176777	0.150	---	309.99	71.13
353010	282.5	6299995	494975	0.180	0.071	444.84	75.74
373008	638.0	4025000	176777	0.180	0.042	807.95	104.92
373044	20177.5	3724998	459619	0.135	0.021	339.82	152.68
453012	6223.0	4724999	247487	0.160	0.042	373.22	41.51
463009	490.3	4857996	---	0.150	---	166.98	13.37
463013	330.6	3975000	106066	0.185	0.007	433.71	123.61
483589	9305.0	5025001	318198	0.150	0.028	313.05	58.27
497083	---	3899999	282843	0.210	0.014	621.28	255.95
533013	1892.7	4674995	459619	0.140	---	273.97	25.35
537409	2505.3	3424998	388909	0.175	0.007	629.43	325.73
553014	4529.4	6199994	212132	0.200	---	413.39	105.45
843803	2360.0	4749998	424264	0.220	0.014	247.51	43.85
893001	2433.8	5675000	388909	0.200	0.014	253.74	141.32
893002	172.0	5025001	1166726	0.200	0.042	73.94	28.31
893015	2405.3	4300002	141421	0.150	0.028	159.33	64.44

Table 15 Site Specific Information and Data - Rigid Pavement  
Construction Variability Study (Continued)

SHRP Section	PCC Thickness	PCC Thickness (Std Dev)	Age (yrs)	Moisture Dry = 1 Wet = 2	Temperature Nonfreeze=1 Freeze=2	Subgrade Fine =1 Coarse=2	IRI
47614	9.670	0.121	7.00	1.0	1.0	1.0	64.87
63010	8.820	0.098	15.00	1.0	1.0	1.0	77.79
63013	9.550	0.152	10.00	1.0	1.0	1.0	104.87
63017	8.070	0.450	13.00	1.0	1.0	2.0	90.89
63042	8.830	0.082	12.00	1.0	1.0	1.0	60.49
123811	9.380	0.214	15.00	2.0	1.0	2.0	0.00
124000	8.080	0.075	17.00	2.0	1.0	2.0	104.32
133015	9.970	0.186	12.00	2.0	1.0	2.0	0.00
133017	9.900	0.063	18.00	2.0	1.0	1.0	78.66
133018	10.000	---	18.00	2.0	1.0	1.0	61.56
163017	10.330	0.361	15.00	1.0	2.0	2.0	100.30
183031	10.160	0.256	15.00	2.0	2.0	1.0	98.36
203015	9.200	0.113	6.00	1.0	2.0	1.0	70.64
233013	10.230	0.413	18.00	2.0	2.0	1.0	133.58
233014	10.270	0.207	18.00	2.0	2.0	2.0	94.59
313028	8.380	0.204	9.00	1.0	2.0	1.0	76.29
353010	7.870	0.082	9.00	1.0	1.0	2.0	0.00
373008	7.870	0.082	17.00	2.0	1.0	1.0	108.71
373044	9.000	0.141	25.00	2.0	1.0	1.0	121.63
453012	9.900	0.063	10.00	2.0	1.0	2.0	0.00
463009	10.800	---	15.00	1.0	2.0	1.0	188.17
463013	9.330	0.103	15.00	1.0	2.0	1.0	100.75
483589	9.870	0.383	30.00	1.0	1.0	1.0	0.00
497083	10.220	0.041	2.00	1.0	2.0	2.0	0.00
533013	8.200	0.155	20.00	1.0	2.0	2.0	117.58
537409	9.330	0.137	3.00	1.0	2.0	2.0	76.44
553014	10.280	0.075	15.00	2.0	2.0	2.0	213.42
843803	8.300	0.167	11.00	2.0	2.0	2.0	164.13
893001	9.030	0.137	17.00	2.0	2.0	2.0	156.70
893002	9.250	0.356	12.00	2.0	2.0	1.0	229.89
893015	8.250	0.176	7.00	2.0	2.0	1.0	88.11

Nonstructural Variables (E)

Age (years)

Traffic (KESALs)

Temperature (freeze versus nonfreeze)

Moisture (wet versus dry)

Regression analyses were completed for the performance IRI and AASHO Serviceability Loss. These quantities were estimated from a relationship developed during SHRP-LTPP (7).

*Longitudinal Roughness in Rigid Pavements, log(IRI)*

The predictive equation for log(IRI) includes main effects of

log(KESALs),  
log(PCC Modulus),  
log(K), and  
log(MOIST)

and interaction effects of

log(KESALs) \* log(K-Var),  
log(AGE) \* log(Mod-Var),  
log(SUBG) \* log(Ts-Var).

The prediction equation is:

$$\begin{aligned} \log(\text{IRI}) = & [-1.79007 - 0.426 * \log(\text{KESALs}) + 0.760 * \log(\text{Mod}) \\ & - 0.170 * \log(K) + 0.250 * \log(\text{Moist})] \\ & - 0.2355 * [\log(K\text{-Var})] + \text{Log}(\text{KESALs}) * [0.0915 * \log(K\text{-Var})] \\ & + \log(\text{AGE}) * [0.0226 * \log(\text{Mod-Var})] \\ & + \text{Log}(\text{SUBG}) * [-0.1955 * \log(\text{Ts-Var})] \end{aligned} \quad \text{Equation 20}$$

where

IRI = pavement roughness as measured in IRI values from SHRP profilometer data  
KESALs = cumulative traffic in thousands of equivalent single axle loads (KESALs) based on historical traffic data  
Mod = surface (PCC layer) modulus  
MOIST = moisture conditions: dry +1, wet +2  
AGE = age of section (years)  
SUBG = subgrade type: fine-grained +1, coarse-grained +2  
Ts = thickness of surface PCC layer (in.)  
K-Var, Mod-Var,  
Ts-Var = variances of K, Mod, and Ts, respectively

These results indicated that pavement roughness generally increased with lower modulus of subgrade reaction ( $K$ ), wetter environments, higher surface modulus, greater pavement age, and greater variation in surface modulus (Mod). It should be noted that the variabilities in  $K$ , Mod, and surface thickness (Ts) all apparently contributed to pavement roughness.

### *AASHO Serviceability Loss*

The predictive equation for log(AASHO Serviceability Loss) contains no main effects but is composed of eight interaction or cross-product terms. Four of the interactions involve mean values of the factors and four involve variances of the factors. The equation includes

$$\begin{aligned} \log(\text{AASHO PSI-Loss}) = & [0.5466] - 0.0292 * [\log(\text{KESALs}) * \log(\text{Temp})] \\ & - 0.1041 * [\log(K) * \log(\text{Ts})] + 0.8024 * [\log(\text{TEMP}) * \log(\text{SUBG})] \\ & + 0.7511 * [\log(\text{SUBG}) * \log(\text{PR})] + \log(\text{KESALs}) * [0.00925 * \log(\text{PR-Var})] \\ & + \log(\text{AGE}) * [0.03333 * \log(K\text{-Var})] + \log(\text{SUBG}) * [-0.3517 * \log(\text{Ts-Var})] \\ & + \log(\text{Ts}) * [0.0774 * \log(\text{Ts-Var})] \end{aligned} \quad \text{Equation 21}$$

with

$$\begin{aligned} R^2 & = 0.9200 \\ \text{RMSE} & = 0.0249 \\ \text{CV} & = 12.2 \\ \text{df} & = 17 \end{aligned}$$

where:

AASHO PSI Loss	= 4.5 - $p$ , where $p$ is present serviceability
KESALs	= cumulative traffic (KESALs) based on historical traffic data
$K$	= modulus of subgrade reaction (pci)
SUBG	= subgrade type: fine-grained +1, coarse-grained +2
TEMP	= temperature zone: nonfreeze +1, freeze +2
Ts	= thickness of surface PCC layer (ins.)
PR	= Poisson's ratio of surface PCC layer
PR-Var, K-Var, Ts-Var	= variances of PR, K, and Ts respectively

The significant consideration in this relationship is the large number of variance terms included. This investigation indicated that the variation in surface layer thickness (Ts), surface layer Poisson's ratio (PR), and modulus of subgrade reaction ( $K$ ) apparently had a significant influence on AASHO Serviceability Loss. These variances translate into primary structural influences (i.e., Ts,  $K$ ) and materials influences (i.e., PR). In addition, the serviceability loss is affected by various combinations of traffic (KESALs), environment (TEMP), and primary structural factors (i.e.,  $K$ , Ts, SUBG and PR).

## Construction Variability in Flexible Pavements

The construction variability factors included in the flexible pavement investigation are identified below. The specific site information and data for the LTPP sections investigated in the flexible pavement construction variability study are presented in Table 16.

### *Flexible Pavement Construction Variability Factors*

#### Distress and Performance Variables (D)

Rutting (Layer)  
Rutting (Deep-Seated)  
IRI  
AASHO PSI-Loss

#### Primary Structural Variables (S)

Surface Layer Thickness (Ts)  
Base Layer Thickness (Tb)  
Structural Number (SN)  
Surface Layer Modulus (Es)  
Base Layer Modulus (Eb)  
Subgrade Modulus (Esg)  
Subgrade Type: (SUBG)

#### Materials Properties (M)

Asphalt Content (AC)

#### Nonstructural Variables (E)

Age (Years)  
Traffic (KESALs)  
Temperature (freeze versus nonfreeze)  
Moisture (wet versus dry)

Regression analyses were completed for the distress and performance variables of rutting (within upper pavement layers), deep-seated rutting (including the subgrade), and AASHO Serviceability Loss. It should be noted that the rut type classification method developed in the Rut Initiation Studies (8) was used here to categorize rutting as either "layer" or "deep-seated." The AASHO Serviceability Loss variable was estimated for the various SHRP-LTPP sections through a relationship developed by Hadley (8) as a part of this study.

### *log(Layer Rutting)*

The predictive equation for log(Layer rutting) includes a main traffic (or log KESALs) effect and four interaction factors (or cross-products) involving traffic and subgrade modulus,

Table 16 Site Specific Information and Data - Flexible Pavement Construction Variability Study

Section ID	SN	Asphalt Content %	Environment			Surface Thickness (Ts,Ins)	Variance in Ts	Base Thickness (Tb,ins)	Variance in Tb	Subgrade Modulus (ksi)
			Density, pcf	-1 dry +1 wet	Moisture Temperature nonfreeze freeze					
052042	3.36	5.10	147.3	+1	-1	5.20	0.9823	6.00	5.4224	10.3
062004	5.21	5.10	152.0	-1	-1	3.40	0.2231	5.30	1.1124	25.4
062051	3.78	4.90	144.6	-1	-1	5.00	0.3257	6.50	4.1630	74.4
062053	5.29	5.10	162.1	-1	-1	4.20	0.0507	8.40	0.7370	45.5
062647	3.68	5.00	150.3	-1	-1	3.70	0.0523	5.30	0.2336	59.1
067491	2.83	5.90	143.3	-1	-1	3.80	0.8216	5.80	5.2274	31.5
068149	2.98	4.70	154.4	-1	-1	4.50	0.3998	5.00	12.8021	43.9
068201	3.50	5.30	134.5	-1	-1	4.50	0.1762	4.80	1.4829	46.1
134112	5.68	5.10	143.9	+1	-1	3.10	0.2153	12.70	8.1944	28.8
134113	5.49	4.90	145.3	+1	-1	3.60	0.2499	11.50	2.9519	35.5
182008	7.15	4.60	147.0	+1	+1	0.60	0.1560	5.40	11.3004	18.0
196150	3.75	5.00	151.1	+1	+1	0.40	0.6188	4.30	1.6989	14.9
223056	5.40	4.00	142.1	+1	-1	3.00	0.5837	8.00	3.6496	33.5
242401	4.90	6.30	139.9	+1	+1	1.30	1.4183	3.60	4.1254	27.5
261013	4.73	4.40	148.8	+1	+1	0.80	0.2347	4.80	27.4253	33.0
271023	5.25	4.40	148.2	+1	+1	1.70	2.2893	4.00	10.7723	40.9
341033	4.66	5.70	161.1	+1	+1	1.20	1.2802	15.00	91.0975	68.8
341638	5.38	4.90	147.7	+1	+1	2.40	0.3743	8.00	1.0064	33.8
371645	4.29	4.10	145.9	+1	-1	1.90	1.3249	7.00	1.1366	32.2
382001	2.88	6.30	145.6	-1	+1	2.40	0.0862	6.30	1.9420	14.1
404154	6.00	4.50	143.7	-1	-1	1.80	1.7226	5.20	0.9659	25.4
479025	3.22	5.00	147.0	+1	-1	2.30	0.2742	3.70	54.4792	12.6
482108	3.92	4.70	144.0	+1	-1	3.00	0.1580	11.60	21.2851	26.1
512004	4.70	5.50	133.0	+1	+1	1.50	0.3281	7.00	0.6857	11.4
562019	5.60	5.70	148.3	-1	+1	3.40	0.1926	10.60	6.1261	28.9
562020	4.55	6.20	146.6	-1	+1	4.20	0.0618	13.50	0.8677	33.3
562037	4.64	5.40	150.1	-1	+1	3.10	0.0924	16.40	4.4342	40.5
567772	3.71	6.90	138.9	-1	+1	2.20	0.1412	13.70	10.9556	23.8
829017	5.89	4.50	151.0	-1	+1	2.00	1.6073	4.00	105.9973	65.9
836454	4.48	4.50	141.0	-1	+1	4.00	0.5420	8.00	1.5060	23.1
872811	4.30	5.10	149.9	+1	+1	1.50	0.0880	8.00	7.6607	36.8
872812	3.86	4.80	155.0	+1	+1	3.00	0.0849	12.00	3.4641	30.9
901802	3.08	5.90	140.0	-1	+1	7.00	0.0599	3.00	0.6529	12.0

Table 16 Site Specific Information and Data - Flexible Pavement Construction Variability Study  
(Continued)

Section ID	Variance Subgrade Modulus	Base Modulus (ksi)	Variance Base Modulus	Surface Modulus 0° psi)	Variance Surface Modulus	Traffic ESALS	Layer Rutting (mm)	Deep Rutting (mm)	IRI	PSI
052042	11.8701	355.5	153886	289	3114	1521	9.18	--	37.63	3.70
062004	31.3426	262.9	619064	575	6355	612	--	--	--	--
062051	89.0934	97.5	124007	957	37924	2992	4.78	--	105.22	2.87
062053	48.0855	632.8	595744	1704	222924	12029	6.92	--	64.97	3.25
062647	43.2318	175.9	574573	1233	247502	1559	--	--	87.85	3.01
067491	30.5061	59.0	196924	797	133543	1661	6.49	--	60.35	3.30
068149	34.0705	281.5	734467	1984	36286	17095	--	--	106.63	2.86
068201	22.2830	710.2	740487	1229	21467	705	--	--	57.83	3.34
134112	36.7736	488.6	4428598	218	1977	9370	--	3.99	79.54	3.12
134113	33.1034	1137.1	18187888	429	14939	5513	--	--	--	--
182008	22.0606	220.8	1092261	734	27233	1474	10.63	--	142.32	2.65
196150	7.8002	67.6	1257250	791	16323	173	--	--	79.68	3.06
223056	29.2816	964.9	1269560	918	12890	1293	4.35	--	--	--
242401	51.2436	171.5	600555	584	4539	252	3.12	--	54.25	3.52
261013	30.3296	228.4	21762156	604	3853	1541	4.40	--	76.77	3.09
271023	19.0591	195.4	43835896	394	551	1537	6.43	--	106.38	2.86
341033	40.2898	22.6	172702	2012	1053931	767	7.11	--	184.09	2.53
341638	39.7382	937.1	1162050	637	19611	1119	5.35	--	60.06	3.44
371645	24.1285	426.6	778791	980	10837	812	5.81	--	49.79	3.59
382001	14.9817	40.8	2688	1083	17726	1495	0.00	8.14	120.03	2.77
479025	199.4281	17.3	2490062	729	21664	316	4.62	--	--	--
482108	22.8828	811.6	11047673	357	4447	132	--	4.73	--	--
512004	3.4096	119.6	4410	1200	10433	1027	3.83	--	85.73	3.15
562019	15.9244	841.7	1930147970	1768	844823	780	--	4.39	84.43	3.04
562020	22.5411	1214.2	388756	1322	4719	946	--	3.76	61.19	3.29
562037	33.8228	649.8	696646	2036	212357	316	--	--	85.81	3.03
567772	21.4200	399.8	954872	1413	153338	228	3.40	--	110.71	2.83
829017	189.1508	4.7	39050	1626	80811	351	--	3.16	67.14	3.22
836454	25.4405	160.0	546688	714	11294	2668	--	9.00	129.71	2.72
872811	44.2166	404.8	253448	888	34417	1549	--	--	73.44	3.27
872812	36.4057	221.3	63448	919	16797	2453	5.54	--	62.97	3.40
901802	0.3652	82.7	3053	414	5475	2459	10.44	--	166.64	2.54

asphalt content and structural number, asphalt content and surface layer thickness, and subgrade modulus and surface layer thickness. The predictive equation is presented below.

$$\begin{aligned} \log(\text{Layer Rutting}) = & - 0.43637 + 0.736 * \log(\text{KESALs}) + \log(\text{KESALs}) \\ & * [-0.187 * \log(\text{Esg}) + \log(\text{AC}) * [0.754 \\ & * \log(\text{SN}) - 1.127 * \log(\text{Ts})] + \log(\text{Esg}) \\ & * [0.240 * \log(\text{Ts-Var})] \end{aligned} \quad \text{Equation 22}$$

$$\begin{aligned} R^2 &= 0.920 \\ \text{RMSE} &= 0.0581 \\ \text{CV} &= 7.9 \end{aligned}$$

where

Layer Rutting	=	Layer rutting in millimeters,
KESALs	=	cumulative traffic in thousands of KESALs based on historical traffic data
Ts	=	thickness of HMAC layer (ins.)
SN	=	structural number
Esg	=	modulus of subgrade (based on FWD data) (ksi)
Ts-Var	=	variance in surface layer thickness (based on FWD data)

From the equation it can be observed that the interaction terms include primarily mean values and that only a single variance term for surface thickness is present. This investigation indicated that increased layer rutting corresponds to

- Increased traffic
- Lower subgrade modulus at any traffic rate and minimum surface thickness variable
- Higher asphalt contents and higher structural numbers
- Thinner surface layers
- Higher surface thickness variation with any subgrade modulus

One of the keys in this instance is the influence of surface thickness variation on layer rutting. Closer control of surface thickness could help prevent rutting.

It is interesting to note that the combination of the interaction terms involving asphalt content could shed light on the compromises that are possible between structural number and surface layer thickness. The combined terms are

$$\log(\text{AC}) * [0.754 * \log(\text{SN}) - 1.127 * \log(\text{Ts})] \quad \text{Equation 23}$$

For a given AC value, an increase in SN (i.e., generally a thicker section) apparently results in the potential for greater rutting because of the positive coefficient associated with log(SN). This effect can be offset, however, by an appropriate selection of Ts because log(Ts) has a negative coefficient. Hence, an appropriate correspondence between SN and Ts values could be beneficial.

### *log(Deep-Seated Rutting)*

The predictive equation for log(Deep-Seated Rutting) does not include any main effects but is composed of four interaction or cross-product terms. Three of these cross-product terms involve variances of subgrade modulus, surface layer thickness, and surface layer modulus. Structural number, temperature zone, subgrade classification, and KESALs are also involved in the interaction terms. The equation is presented below.

$$\begin{aligned} \log(\text{Rut-Deep}) = & 1.3817 + 1.371 * [\log(\text{SUBG}) * \text{Log}(\text{TEMP})] \\ & - \log(\text{SN}) * [0.449 * \log(\text{Esg-Var})] + \log(\text{AGE}) \\ & * [0.211 * \log(\text{Ts-Var})] - \log(\text{KESALs}) \\ & * [0.0106 * \log(\text{Es-Var})] \end{aligned} \quad \text{Equation 24}$$

R <sup>2</sup>	= 0.841
RMSE	= 0.0800
CV	= 11.0
number sites	= 11

where

Rut-Deep	= deep seated rutting in millimeters
SN	= structural number
AGE	= age of section in years
KESALs	= cumulative traffic in thousands (KESALs) based on historical traffic data
SUBG	= subgrade general classification: fine grained +1, coarse grained +2
TEMP	= temperature zone: nonfreeze +1; freeze +2
Es-Var, Ts-Var, and Esg-Var	= variances in surface layer modulus (Es), surface layer thickness (Ts), and subgrade modulus (Esg).

This investigation indicated that deep-seated rutting corresponds to

- Colder locations with coarse-grained soils
- Lower structural numbers
- Greater age and higher variation in surface layer thickness
- Lower variation in surface layer modulus at any traffic rate

The phenomenological difference between layer rutting and deep-seated rutting can be observed in the impact of the structural number factor. Layer rutting is more likely in pavements with higher structural numbers, while deep-seated rutting is less likely in similar pavements with high structural numbers.

## *AASHO Serviceability Loss*

The predictive equation for log(4.2-p) contains no main effects but does include eight interaction terms. Four of these cross-product terms include variance terms for subgrade modulus, surface layer thickness, and surface modulus. The equation for this performance variable is presented below.

$$\begin{aligned} \log(4.2 - p) = & - 0.10471 + \log(\text{TEMP}) * [0.402 * \log(\text{AGE}) + 1.953 \\ & * \log(\text{SUBG})] + \log(\text{MOIST}) * [4.72 * \log(\text{SN}) - 1.360 \\ & * \log(\text{SUBG})] + \log(\text{KESALs}) * [0.028 * \log(\text{Es-Var})] \\ & - \log(\text{Ts}) * [0.073 * \log(\text{Es-Var})] - \log(\text{Esg}) \\ & * [0.317 * \log(\text{Esg-Var})] + \log(\text{MOIST}) * [0.472 \\ & * \log(\text{Ts-Var})] \end{aligned} \quad \text{Equation 25}$$

$$\begin{aligned} R^2 &= 0.7900 \\ \text{RMSE} &= 0.0542 \\ \text{CV} &= 37.5\% \end{aligned}$$

where

AGE	=	age of section in years
KESALs	=	cumulative traffic in thousands (KESALs) based on historical traffic data
Ts	=	surface layer thickness (ins.)
Es	=	surface layer modulus (from FWD data) (ksi)
Esg	=	subgrade modulus (from FWD data)
MOIST	=	environmental conditions: dry +1, wet +2,
TEMP	=	environmental conditions: nonfreeze +1, freeze +2
SUBG	=	subgrade assignment as: fine-grained +1, coarse-grained +2

Temperature zone, age, subgrade classification, moisture conditions, structural number, KESALs, and subgrade modulus are also included in the equation.

This investigation indicated that greater serviceability loss corresponds to

- Older pavements
- Higher structural numbers
- Higher traffic and higher surface modulus variance
- Thinner surface layers
- Lower subgrade modulus with associated subgrade modulus variance
- Greater surface thickness variance in the wetter zones

It is important to note that mean structural number and surface layer thickness are influential and apparently affect the amount of serviceability loss. The variances of surface layer modulus and surface layer thickness likewise can influence serviceability. Because all these items are related to the structural/materials design process, it appears possible to identify

specification controls, construction methods, and other measures that could be used to "harness" these factors and reduce pavement serviceability loss.

## **Conclusions**

This investigation of materials and construction variability within rigid and flexible SHRP-LTPP pavement sections successfully identified significant effects, interactions, and variances of effects that can influence pavement distress and performance.

The results represent an initial effort in defining construction variability and should be expanded to include more LTPP sections, as well as other distress and performance variables as they become available in the LTPP database.

The analytical approach used in this study (6) appears to be valid and should be used in future analytical efforts to define construction variability.

# **Rutting Initiation Studies**

## **Introduction**

The development of rutting in flexible pavements is an expected phenomenon which impacts pavement serviceability and influences rehabilitation decisions. The rutting phenomenon is a complicated one and can develop within pavement layers (i.e., layer rutting) due to layer densification and/or material instability (shoving) or within the total pavement structure including the subgrade soil (i.e., deep-seated rutting). The definition of the source or cause of initiation of rutting within a pavement structure is needed to enhance flexible pavement design and evaluation strategies.

An evaluation of the distortion in a pavement cross profile can not only be used to establish pavement rut depth but also to provide insight into the underlying cause and/or location of initiation of the rutting phenomenon. The availability of PASCO Cross Profile data for all SHRP flexible pavement sections offers an excellent opportunity to investigate the rutting phenomenon, particularly since detailed section information on pavement structure, environmental conditions, material values, traffic and geographic information is available within the LTPP National Pavement Performance Database (or NPPDB).

This data analysis effort was undertaken to develop information on factors influencing the type of rutting (i.e. within layers or deep-seated), and to investigate the source of rut initiation and distortion of the pavement cross profile which develops within a pavement structure. The factors under investigation included prevailing moisture and temperature conditions, subgrade types, traffic and layer thicknesses. Regression equations relating the amount of rutting and extent (or type) of rutting to the various factors were developed.

## **Rut Depth Estimation and Cross Profile Distortion**

### *Introduction*

A majority of the raw, transverse profile data for SHRP GPS sections is being collected in an automated fashion using the PASCO Data Collection Vehicle (13). In addition, cross profile information for some of the GPS Sections is generated using the FACE DIPstick®.

The data generation package, PADIAS, developed by PASCO (14), includes a method for estimating rut depths from cross profile data. In many instances, however, the PASCO technique does not conform with the classic straight edge measurement method. Because of

this situation, a technique (see Figure 6) was developed to estimate rut depths by simulating placement of straight edges of variable length upon the existing PASCO cross profile data (15,16). In addition, a pavement distortion assessment method was developed as an aid in identifying possible causes and/or location of rutting (15). The pavement distortion possibilities are presented in Figure 7.

### *Analytical Approach*

Several parameters were considered and subsequently selected to investigate their influence on initiation and extent of rutting. Since distortion of pavements can be caused by consolidation of one or more of the structural layers and/or the subgrade, rutting can consequently develop in the subgrade, base or surface layers. This pavement distress can arise from deformation under traffic loading and as surface distortion influenced by climatic conditions as well as the moisture content of the subgrade.

This analysis of rutting included an investigation of a number of causative factors including the following:

#### Structural Number (SN)

The SN is an index number representative of pavement structural capacity that reflects the influence of material type and thickness of the pavement layers. The structural number was generated by a program developed for estimating the results from data obtained during the on-site drilling program.

#### Structure (ST)

Four types of pavement structure were considered.

- Asphalt concrete over granular base (AC/GB)
- Asphalt concrete over stabilized base (AC/SB)
- Asphalt concrete overlay of asphalt concrete (AC/AC)
- Asphalt concrete overlay of portland cement concrete (AC/PCC)

#### Surface Thickness (TS)

The thickness of the surface layer was defined from drilling and sampling results for the particular SHRP LTPP Section.

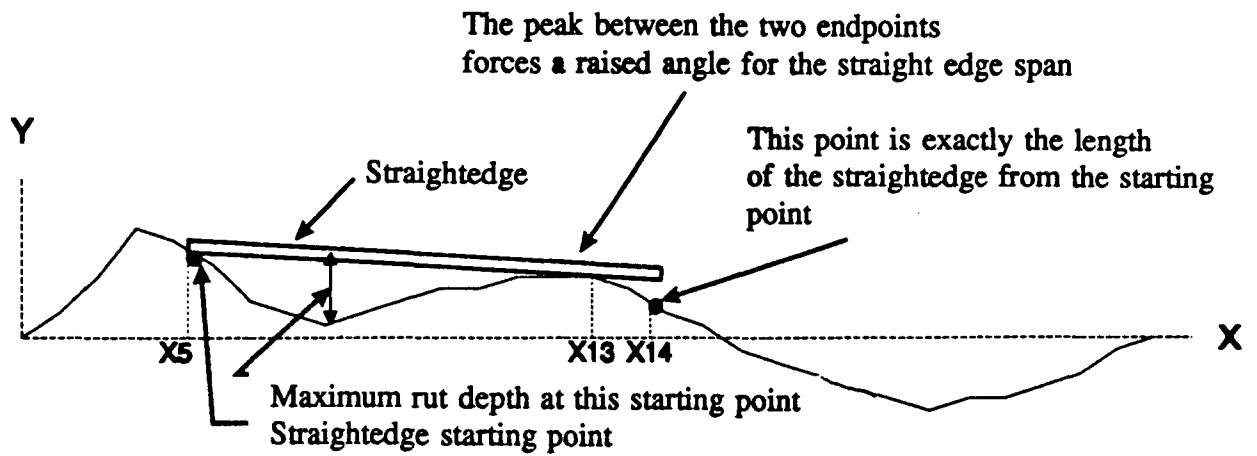
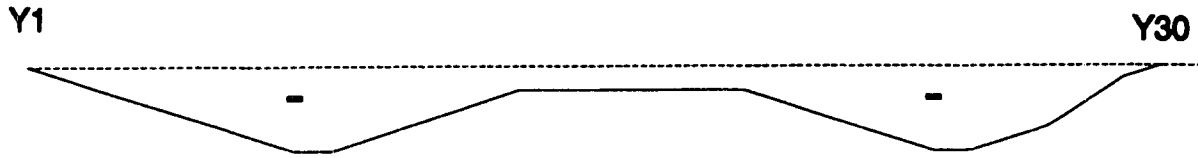


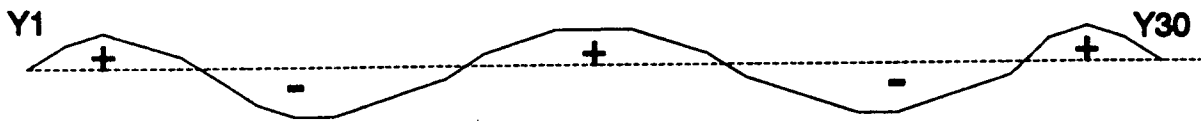
Figure 6 Example of Intermediate Point to Higher Elevation Between Starting Point (X5) and Ending Point (X14) of a Straightedge

Net distortion is negative.  
(no + values)



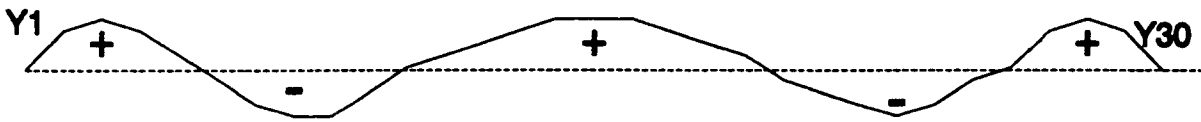
Case 1: Deep Subgrade Rutting

Net Distortion is near zero.



Case 2: Rutting Within Pavement Layer

Net distortion is positive.



Case 3: Shoving Within Upper Layer

Figure 7 Pavement Distortion Possibilities

## Type of Subgrade (SG)

The subgrade type was defined as either FINE or COARSE based on inventory data acquired in the GPS studies.

## Modulus (E)

The modulus was estimated for every layer from FWD deflection data. The estimates were developed for a pavement structure characterized as a three layer system with the three modulus values  $E_s$ ,  $E_b$  and  $E_s$  identifying the modulus of subgrade, base and surface layers respectively.

## Moisture Condition (M)

The moisture condition reflects the moisture content expected in the subgrade soil for that LTPP section and was categorized as either WET for high moisture content or as DRY for a low moisture content. The weather condition classifications are based on the SHRP environmental regions (see Figure 8).

## Environmental Condition (C)

The environmental condition characterizes the climatic state for the pavement sections and represents the influence of weather on the surface distortion caused during rutting. This parameter was classified as either a freeze or nonfreeze situation in accordance with the SHRP-LTPP environmental regions (Figure 8).

## Traffic Rate (TF)

The amount of traffic was defined in KESALs (i.e., thousands of Equivalent Single Axle Loads) and was obtained from the State Highway Agency (SHA) historical traffic data.

### *Selected SHRP-LTPP Sections*

A total of sixty sections was investigated forming a matrix of 12 factor fields for 60 observations. The sections were selected from the four SHRP regions (Figure 8) to provide a uniform distribution of pavement characteristics across the United States.

A comprehensive listing of the LTPP sections including extracted, generated, and derived data is presented in Table 17 for the flexible pavement structures and Table 18 for the composite (HMAC overlay of a PCC Pavement) pavement sections.

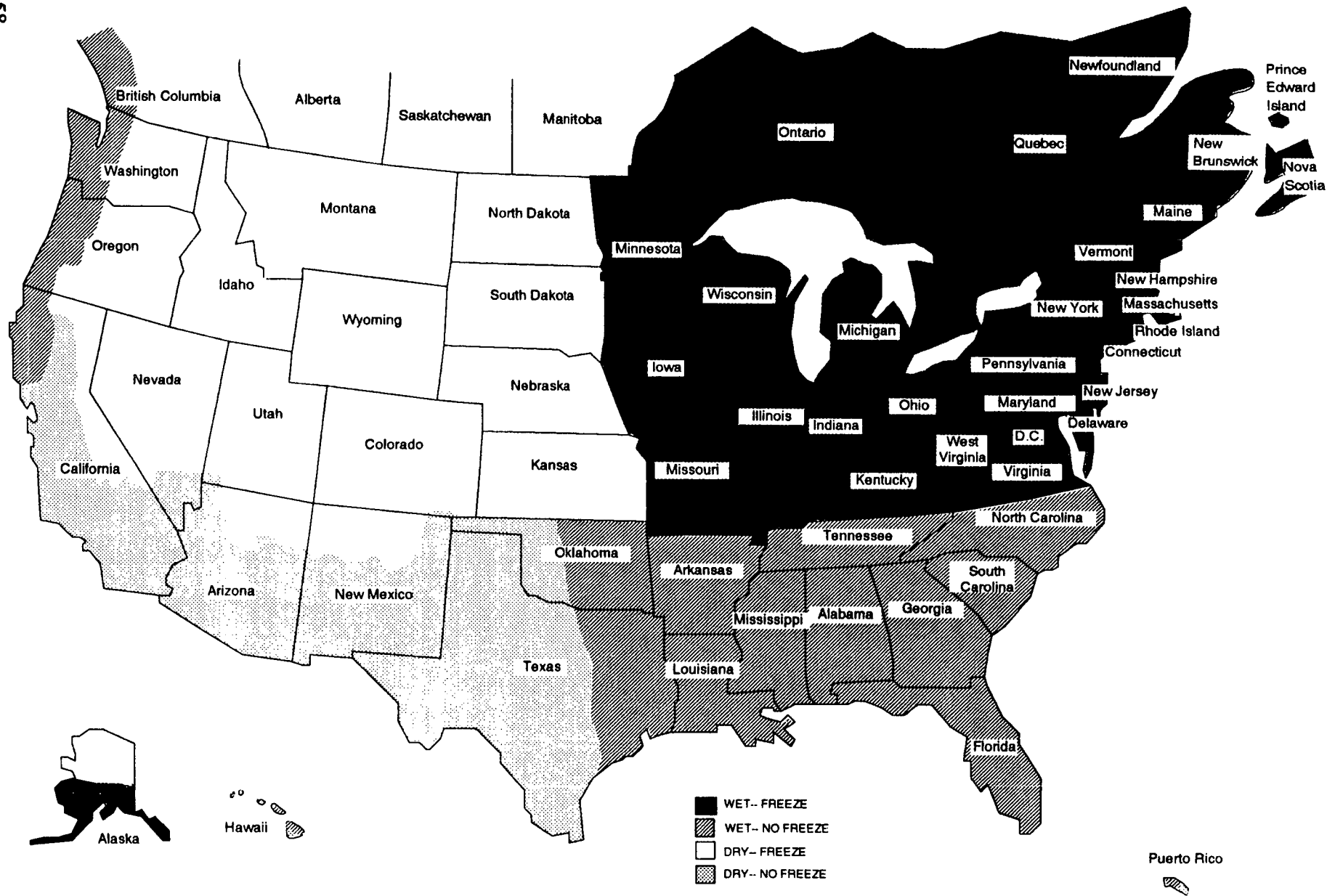


Figure 8 Environmental Zones for SHRP-LTPP Experiments

Table 17. List of LTPP Sections for the Flexible Pavement Structures

SITE LOCATION		SITE SPECIFIC INFORMATION AND CONDITIONS						SURFACE LAYER CHARACTERISTICS					SUBGRADE	AREAL DISTORTION			RUTTING	
SHP SECTION	STATE SHA	STRUCT TYPE	STRUCT NUMBER	SUBG TYPE	SUBG MOIST	ENVIRON CONDITION	CUMUL KESALs	THICK (ins)	% ASPH	% AIR VOIDS	DENS LB/CF	MODULUS KSI	MODULUS KSI	DOWN (-)	UP (+)	NET (+ or -)	TYPE	DEPTH (mm)
41062	ARIZONA	AC/AC	4.97	COARSE	DRY	NO FREEZE	1401	5.4	5.3	7.2	138.2	562.4	34.90	1525	4974	3449	SHOVING	4.68
41065	ARIZONA	AC/AC	5.10	COARSE	DRY	NO FREEZE	1384	4.8	5.6	10.7	140.0	997.6	23.49	12676	365	-12311	DEEP	5.82
52042	ARKANSAS	AC/SB	3.36	FINE	WET	NO FREEZE	1521	2.0	5.1	1.7	147.3	289.1	10.26	12937	3083	-9855	LAYER	9.18
53071	ARKANSAS	AC/AC	6.64	FINE	WET	NO FREEZE	1758	1.5	4.5	3.8	147.2	523.2	36.25	2913	2548	-365	LAYER	4.40
62004	CALIFORNIA	AC/SB	5.21	FINE	DRY	NO FREEZE	612	3.4	5.1	6.0	152.0	497.6	35.10	813	13268	12455	HEAVING	4.35
62051	CALIFORNIA	AC/SB	3.78	COARSE	DRY	NO FREEZE	2992	5.0	4.9	7.3	144.6	768.8	40.65	8665	1395	-7270	LAYER	4.78
62053	CALIFORNIA	AC/SB	5.29	FINE	DRY	NO FREEZE	12029	4.2	5.1	2.5	162.1	1491.3	29.98	7112	4537	-2576	LAYER	6.92
62647	CALIFORNIA	AC/SB	3.68	COARSE	DRY	NO FREEZE	1559	3.7	5.0	2.3	150.3	1521.9	31.98	2175	7667	5492	SHOVING	4.24
67491	CALIFORNIA	AC/SB	2.83	COARSE	DRY	NO FREEZE	1661	3.8	5.9	5.1	143.3	749.2	22.88	7182	8171	989	LAYER	6.49
68149	CALIFORNIA	AC/SB	2.98	COARSE	DRY	NO FREEZE	17095	4.5	4.7	5.6	154.4	1903.3	32.32	1618	18534	16916	HEAVING	4.38
68201	CALIFORNIA	AC/SB	3.50	COARSE	DRY	NO FREEZE	705	4.5	5.3	11.1	134.5	1107.5	33.55	1754	5486	3732	SHOVING	2.66
124108	FLORIDA	AC/AC	5.03	COARSE	WET	NO FREEZE	389	3.4	5.5	5.5	145.0	1549.5	20.10	4187	6550	2363	LAYER	8.80
124112	GEORGIA	AC/SB	5.68	COARSE	WET	NO FREEZE	9370	3.1	5.1	4.7	143.9	146.7	22.27	8239	776	-7463	DEEP	3.99
124113	GEORGIA	AC/SB	5.49	COARSE	WET	NO FREEZE	5513	3.6	4.9	4.3	145.3	380.5	25.56	1155	8448	7293	SHOVING	3.38
182008	INDIANA	AC/SB	7.15	FINE	WET	FREEZE	1474	0.6	4.6	6.9	147.0	670.6	22.02	9077	6508	-2569	LAYER	10.63
196150	IOWA	AC/SB	3.75	FINE	WET	FREEZE	173	0.4	5.0	1.9	151.1	848.3	12.96	1763	13861	12098	HEAVING	6.83
201009	KANSAS	AC/AC	4.54	COARSE	DRY	FREEZE	472	2.4	4.6	4.8	144.0	955.5	22.09	5302	3014	-2288	LAYER	6.18
223056	LOUISIANA	AC/SB	5.40	FINE	WET	NO FREEZE	1293	3.0	4.0	6.4	142.1	819.2	24.43	3653	1179	-2475	LAYER	4.35
242401	MARYLAND	AC/SB	4.90	FINE	WET	FREEZE	252	1.3	6.3	7.7	139.9	510.8	17.95	3921	1235	-2686	LAYER	3.12
261013	MICHIGAN	AC/GB	4.73	COARSE	WET	FREEZE	1541	0.8	4.4	4.7	148.8	518.1	19.55	1620	5363	3743	LAYER	4.40
271023	MINNESOTA	AC/GB	5.25	COARSE	WET	FREEZE	1537	1.7	4.4	4.9	148.2	333.8	23.56	8610	1653	-6957	LAYER	6.43
307076	MONTANA	AC/AC	6.25	FINE	DRY	FREEZE	191	4.5	6.5		146.0	3708.5	10.41	11375	445	-10930	DEEP	7.04
321030	NEVADA	AC/AC	3.59	COARSE	DRY	NO FREEZE	920	6.8	5.1	2.9	148.9	533	19.05	7018	1120	-5898	DEEP	5.64
322027	NEVADA	AC/AC	3.96	COARSE	DRY	FREEZE	4577	4.8	5.5	4.2	143.2	1858	19.98	15848	682	-15166	DEEP	9.87
327000	NEVADA	AC/AC	3.12	COARSE	DRY	FREEZE	4374	3.9	5.3	6.2	141.7	1686.5	27.28	13573	540	-13033	DEEP	5.55
341033	NEW JERSEY	AC/SB	4.66	COARSE	WET	FREEZE	767	1.2	5.7	3.3	161.1	1885.4	35.52	5762	2842	-2920	LAYER	7.11
341034	NEW JERSEY	AC/AC	4.98	FINE	WET	FREEZE	706	3.4	5.4	4.1	150.0	1178.9	21.11	1360	10459	9099	HEAVING	4.83
341638	NEW JERSEY	AC/SB	5.38	COARSE	WET	FREEZE	1119	2.4	4.9	5.1	147.7	565.6	24.75	4555	4353	-202	LAYER	5.35
371645	N. CAROLINA	AC/SB	4.29	COARSE	WET	NO FREEZE	812	1.9	4.1	4.2	145.9	875.5	23.28	6900	960	-5940	LAYER	5.81
382001	N. DAKOTA	AC/SB	2.88	COARSE	DRY	FREEZE	1495	2.4	6.3	2.9	145.6	1083.3	13.51	19542	266	-19276	DEEP	8.14
404154	OKLAHOMA	AC/SB	6.00	FINE	DRY	NO FREEZE	631	1.8	4.5	7.1	143.7	309.7	21.17	565	14216	13651	HEAVING	3.74
404163	OKLAHOMA	AC/AC	4.63	FINE	DRY	NO FREEZE	1994	5.3	4.1	4.6	149.2	972.5	21.67	22203	257	-21946	DEEP	6.62
404165	OKLAHOMA	AC/AC	3.35	COARSE	DRY	NO FREEZE	577	2.7	4.6	5.3	146.6	978.6	20.52	14335	355	-13980	DEEP	6.73
479025	TENNESSEE	AC/SB	3.22	COARSE	WET	NO FREEZE	316	2.3	5.0	6.2	147.0	577.9	55.25	3465	6416	2951	LAYER	4.62
482108	TEXAS	AC/SB	3.92	FINE	WET	NO FREEZE	132	3.0	4.7	5.2	144.0	329.3	21.49	13162	221	-12941	DEEP	4.73
512004	VIRGINIA	AC/SB	4.70	COARSE	WET	FREEZE	1027	1.5	5.5	1.9	133.0	1210.2	12.31	2553	3348	795	LAYER	3.83

Table 17. List of LTPP Sections for the Flexible Pavement Structures, Continued

SITE LOCATION		SITE SPECIFIC INFORMATION AND CONDITIONS						SURFACE LAYER CHARACTERISTICS					SUBGRADE	AREAL DISTORTION			RUTTING	
SHP SECTION	STATE SHA	STRUCT TYPE	STRUCT NUMBER	SUBG TYPE	SUBG MOIST	ENVIRON CONDITION	CUMUL KESALs	THICK (in)	% ASPH	% AIR VOIDS	DENS LB/CF	MODULUS KSI	MODULUS KSI	DOWN (-)	UP (+)	NET (+ or -)	TYPE	DEPTH (mm)
541640	W. VIRGINIA	AC/AC	7.47	COARSE	WET	FREEZE	654	2.5	5.1	6.0	142.9	779.7	25.03	6104	1969	-4135	LAYER	5.04
562019	WYOMING	AC/SB	5.60	COARSE	DRY	FREEZE	780	3.4	5.7	2.3	148.3	1584.8	22.52	9414	185	-9229	DEEP	4.39
562020	WYOMING	AC/SB	4.55	COARSE	DRY	FREEZE	946	4.2	6.2	3.0	146.6	1321.9	33.82	15024	195	-14829	DEEP	3.76
562037	WYOMING	AC/SB	4.64	COARSE	DRY	FREEZE	316	3.1	5.4	2.1	150.1	1791	27.24	5304	897	-4407	SHOVING	3.18
567772	WYOMING	AC/SB	3.71	COARSE	DRY	FREEZE	228	2.2	6.9	4.0	138.9	1261.1	17.36	5996	3034	-2962	LAYER	3.40
829017	B COLUMBIA	AC/GB	5.89	COARSE	DRY	FREEZE	361	2.0	4.5	3.9	151.0	1455.6	33.61	16338	389	-15948	DEEP	3.16
836454	MANITOBA	AC/SB	4.48	FINE	DRY	FREEZE	2668	4.0	4.5		141.0	684.3	19.12	20664	1746	-18918	DEEP	9.00
872811	ONTARIO	AC/SB	4.30	FINE	WET	FREEZE	1549	1.5	5.1	3.9	149.9	792.5	26.20	416	10535	10120	HEAVING	4.12
872812	ONTARIO	AC/SB	3.86	FINE	WET	FREEZE	2453	1.5	4.8	1.6	155.0	918.5	30.86	2152	5687	3535	LAYER	5.54
901802	SASKATCH	AC/GB	3.08	COARSE	DRY	FREEZE	2459	7.0	5.9	7.9	140.0	422.6	9.94	3754	11773	8018	LAYER	10.44

Table 18. List of LTPP Sections for the Composite Pavement Sections

SITE LOCATION		SITE SPECIFIC INFORMATION AND CONDITIONS						HMAC CHARACTERISTICS				AREAL DISTORTION			RUTTING	
SHRP SECTION	STATE SHA	STRUCT TYPE	PCC TH (ins)	SUBG TYPE	SUBG MOIST	ENVIRON CONDITION	CUMUL KESALS	THICK (ins)	% ASPH	% AIR VOIDS	DENS LB/CF	DOWN (-)	UP (+)	NET (+ or -)	TYPE	DEPTH (mm)
177937	ILLINOIS	AC/PCC	9.2	FINE	WET	FREEZE	447	1.5	4.3	7.4	145.1	11271	375	-10896	SHOVING	5.05
267072	MICHIGAN	AC/PCC	9.2	COARSE	WET	FREEZE	3039	2.4	4.6		145.0	1753	5874	4121	LAYER	4.48
277090	MINNESOTA	AC/PCC	7.8	FINE	WET	FREEZE	2259	0.8	4.2	6.1	144.3	477	8656	8179	SHOVING	2.68
317017	NEBRASKA	AC/PCC	7.9	FINE	DRY	FREEZE	399	3.2	5.2	1.8	146.9	1021	20570	19549	SHOVING	6.66
397021	OHIO	AC/PCC	9.0	FINE	WET	FREEZE	7177	1.2	5.3	5.5	150.4	2748	2166	-582	LAYER	3.50
283097	MISSISSIPPI	AC/PCC	10.9	FINE	WET	NO FREEZE	1687	1.6	5.6		142.5	998	8197	7199	SHOVING	3.02
287012	MISSISSIPPI	AC/PCC	9.4	FINE	WET	NO FREEZE	2031	2.4	5.3	2.9	145.1	20859	1647	-19212	SHOVING	16.72
457019	S. CAROLINA	AC/PCC	6.9	COARSE	WET	NO FREEZE	553	2.0	5.1	6.8	145.8	3629	5638	2009	LAYER	3.24
487165	TEXAS	AC/PCC	10.2	FINE	WET	NO FREEZE	3125	1.4	5.8	0.7	146.5	23370	1386	-21984	SHOVING	12.65
87035	COLORADO	AC/PCC	8.4	FINE	DRY	FREEZE	3431	4.8	5.7	1.9	148.4	25206	365	-24841	SHOVING	15.06

## Definition of Rutting Type

The pavement cross profiles vary from one section to another reflecting different rut depth values, as well as, varying total pavement distortion. The rutting at each section was basically classified as deep-seated or layer type. This classification was based on the amount of distortion for each pavement section, established from an evaluation of the PASCO cross profile data. The deep-seated distortion would normally be indicative of a subgrade breakdown, while the surface distortion type would be related to distress in the surface and/or base layers. This distortion classification was defined for each pavement section and was included in the analysis as a rutting type parameter (RT).

The type of rutting was inferred from the relative amounts of pavement distortion using the criteria defined in Figure 7. The amounts of uplift (+ distortion) and consolidation (- distortion) were developed for the cross-section profile of all the SHRP-LTPP sections and are presented under the "rutting characteristics" heading of Tables 17 and 18.

The deep-seated case will be identified as rutting type 1 while the intermediate and the surface cases will be classified as type 2. In addition the rut type may be classified as case 3 (i.e. shoving within the upper layer) or case 4 (i.e., heaving). Heaving is identified with a greater amount of uplift (+) than consolidation (i.e., > 7 to 1).

### *Type of Rutting*

The type of rutting (i.e., layer or deep-seated) was analyzed utilizing linear regression techniques to identify those variables influencing their development. The analysis was completed for an HMAC surface layer over a stabilized base, an HMAC surface layer over a granular base and an HMAC overlay of an original HMAC surface layer. It should be noted that deep rutting developed in only one of the five sections with an HMAC surface layer over a granular base.

### HMAC on Stabilized Base

The source of rutting regression equation for HMAC on a stabilized base is presented in Figure 9 along with the particulars associated with the equation. The dependent variable is RT which approaches a unit negative (-1) value for a "deep-seated" rutting condition and a unit positive (+1) value for a "layer" rutting condition.

The equation incorporates four independent variables including surface thickness, TS, temperature (C) and moisture (M) zones, and surface layer modulus. The signs (i.e. + or -) for the coefficients of these variables provide an indication of the impact of the variables on type of rutting (i.e. layer or deep-seated) expected to develop. For example, deep-seated rutting (RT = -1) would more likely develop with increased surface thickness and surface modulus in a pavement section. There is an interaction (or cross product) between the temperature and moisture zones,  $M \times C$ , which must also be considered.

## Source of Rutting

### HMAC on Stabilized Base

$$R_T = 0.5 - 0.36(T_s - 2.73) - .42(E_s - 750) \\ - 0.55(C) + 0.55(M * C)$$

where

$R_T$  = Rut Type layer +1, deep -1

$T_s$  = Surface Thickness, inches

$E_s$  = Surface Modulus, million psi

$C$  = Temperature zone freeze +1, nonfreeze -1

$M$  = Moisture condition wet +1, dry -1

$$R^2 = 0.65$$

$$RMSE = 0.64$$

$$CV = 173.9$$

18 sites

Figure 9. Source of Rutting - HMAC on Stabilized Base

In general an increase in surface thickness ( $T_s$ ) or surface modulus ( $E_s$ ) tends to produce "deep-seated" rutting when the negative coefficients (-0.36 and -0.42) are considered. In addition, sections located within the colder (i.e.  $C = +1$ ) and drier (i.e.  $M = -1$ ) climatic zones would tend to develop deep-seated rutting (i.e.  $-0.55(1) + 0.55(-1 \times +1) = -1.10$ ). On the other hand the sections within the warmer (i.e.  $C = -1$ ) and drier (i.e.  $M = -1$ ) climatic zones would tend to develop rutting within the layers.

An interesting phenomenon could exist within the colder ( $C = +1$ ) and wetter ( $M = +1$ ) climatic zones since the main effects of temperature ( $C$ ) could essentially cancel the effect of the interaction between temperature and moisture (i.e.,  $M \neq C$ ). In this latter case the surface layer thickness becomes the apparent dominant effect.

The combination of factors included within the equation which would tend to produce "layer" and "deep-seated" rutting are presented in Table 19.

### HMAC on Granular Base

The rutting source regression equation for HMAC on a granular base is presented in Figure 10 along with the characteristics associated with the equation. The equation incorporates the two independent main effects of moisture ( $M$ ) condition and pavement structural number ( $SN$ ). The value of the moisture coefficient (+0.63) indicates that moisture exerts a significant influence on rut type in wet environments since it results in a  $R_T$  value of +1 (layer rutting) for structural numbers of about 4.7. Deep-seated rutting ( $R_T$  of -1) could be expected for pavement sections located in dry environs with structural numbers approaching 6.0.

The combination of factors included within the  $R_T$  equation which would tend to produce "layer" and "deep-seated" rutting are presented in Table 20.

### HMAC Overlay of HMAC

The rutting equation source for a flexible pavement overlay is presented in Figure 11. The equation was developed from the results of ten LTPP sections and incorporates two independent main effects: moisture condition ( $M$ ) and overlay layer thickness,  $T_{OL}$ . In the equation, the moisture coefficient of +0.63 implies that the moisture condition has a significant direct influence on type of rutting developed; however, the influence of overlay thickness must also be considered in order to produce a near unit value (+ or -) for the dependent rut type term. The approximate combinations of moisture and overlay thickness which tend to produce "deep-seated" and "layer" rutting are presented in Table 21.

Table 19. Rut Type Combinations - HMAC on Stabilized Base

	$R_T$	Surface Modulus Es, Ks	Temperature C	Moisture M	Surface Thickness $T_s$
Deep	-1	500	+ (freeze)	-1 (dry)	$\geq 4.1$
	-1	500	+1 (freeze)	+1 (wet)	$\geq 7.2$
	-1	750	+1 (freeze)	-1 (dry)	$\geq 3.8$
	-1	750	+1 (freeze)	+1 (wet)	$\geq 6.9$
		1000	+1 (freeze)	-1 (dry)	$\geq 3.5$
		1000	+1 (freeze)	+1 (wet)	$\geq 6.6$
Layer	+1	500	-1 (nonfreeze)	-1 (dry)	$\leq 4.7$
	+1	500	-1 (nonfreeze)	+1 (wet)	$\leq 1.6$
	+1	750	-1 (nonfreeze)	-1 (dry)	$\leq 4.4$
	+1	750	-1 (nonfreeze)	+1 (wet)	$\leq 1.3$
	+1	1000	-1 (nonfreeze)	-1 (dry)	$\leq 4.1$
	+1	1000	-1 (nonfreeze)	+1 (wet)	$\leq 1.0$

Source of Rutting

HMAC on Granular Base

$$R_T = 0.47 - 0.68(SN - 4.72) + 0.63(M)$$

where

$R_T$  = Rut Type  
layer +1,  
deep -1

SN = Structural Number

M = Moisture Condition  
wet +1, dry -1

$R^2 = 0.97$   
RMSE = 0.225  
5 sites

Figure 10. Source of Rutting on Granular Base

Table 20. Rut Type Combinations - HMAC on Granular Base

Rut Type	R <sub>T</sub>	Moisture, M	SN
Deep	-1	-1 (dry)	≥ 6.0
	-1	+1 (wet)	≥ 7.8
Layer	+1	-1 (dry)	≤ 3.0
	+1	+1 (wet)	≤ 4.9

## Source of Rutting

### HMAC Overlay of HMAC

$$R_T = 0 + 0.63(M) - 0.25(T_{OL} - 3.87)$$

where

$R_T$  = Rut Type  
layer +1,  
deep -1

$T_{OL}$  = Overlay Thickness, inches

$M$  = Moisture Condition  
wet +1, dry -1

$R^2 = 0.76$   
 $RMSE = 0.56$   
10 sites

Figure 11. Source of Rutting - HMAC Overlay of HMAC

Table 21. HMAC Overlay of HMAC

Rut Type	$R_T$	Moisture, M	$T_{OL}$
Deep	-1	-1 (dry)	$\geq 5.4$
Layer	+1	+1 (wet)	$\leq 2.4$

## Shoving Distortion (Case 3)

Shoving within the upper layer was observed in four of the 26 sections included in the analysis of the flexible pavements with stabilized bases. In these four instances the subgrade soil was classified by inventory data as coarse grained. It is important to note that none of the flexible pavements with granular bases were found to exhibit shoving distortion.

### *Rut Prediction Equations*

Once the rut type was designated for each SHRP-LTPP sections included in this study, equations for predicting the magnitude of each type of rutting (i.e. "layer" or "deep-seated") for each pavement type were developed using simple linear regression techniques.

### HMAC on Granular Base

Equations for estimating rut depth (in mm) for "layer" and "deep-seated" rut distortion are presented in Figure 12. Both equations have relatively high  $R^2$  values (0.80 for deep-seated and 0.85 for layer) but were developed from a small number of sites (4 and 3 respectively). These equations should therefore be considered as preliminary and should eventually be confirmed with additional results.

Based on these results, the magnitude of rut depth in the "deep-seated" category is primarily a function of the structural number (SN) or structural capacity of the section. An increase in SN would produce lesser rut depths, which a decrease in SN would yield greater rut depths. Therefore, the composite effect of the pavement structure influences the magnitude of rutting throughout the total pavement structure (including the subgrade).

The magnitude of "layer" rut depth which develops in the upper layers of a pavement structure is primarily related to the thickness of the top pavement layer. As a result, greater rut depths are expected for a pavement with a thicker surface layer, while lesser rut depths are anticipated for a pavement with a thinner surface layer.

### HMAC on Stabilized Base

The equations for estimating rut depth (in mm) for "layer" and "deep-seated" distortion are presented in Figure 13. Both equations have reasonable  $R^2$  value (i.e., 0.83 for deep-seated and 0.62 for layer) and were developed from a total of seventeen sites. These equations should also be considered preliminary and should be confirmed when additional results are available.

From this study it was found that the magnitude of rut depth in the "deep-seated" category is a function of the subgrade modulus and thickness of the HMAC surface layer. From the

## Results

### HMAC on Granular Base

Deep             **$RD = 6.3 - 2.4(SN - 4.72)$**

SN = Structural Number

$$R^2 = 0.80$$

$$RMSE = 1.4$$

4 Sites

Layer             **$RD = 7.1 + 0.8(T_s - 2.7)$**

$T_s$  = Surface Thickness

$$R^2 = 0.85$$

$$RMSE = 1.2$$

3 Sites

Figure 12. Rut Depth Regression Equations - HMAC on Granular Base

## Results

### HMAC on Stabilized Base

Deep  $\mathbf{RD = 5.7 - .45(E_{SG} - 22.1) + 2.82(T_S - 3.35)}$

$E_{SG}$  = Subgrade Modulus, ksi

$T_S$  = Surface Thickness, inches

$R^2 = 0.81$

$RMSE = 1.29$

6 Sites

Layer  $\mathbf{RD = 6.1 - 1.69(AC - 5.16) - 0.05(E_{SG} - 25.5)}$

$\mathbf{+ 0.302(AGE = 10.9)}$

$AC$  = Asphalt Content, %

$E_{SG}$  = Surface Modulus, ksi

$R^2 = 0.62$

$RMSE = 1.6$

12 Sites

Figure 13. Rut Depth Equations - HMAC on Stabilized Base

"deep-seated" rut equation, it can be observed that lower subgrade moduli combined with thicker surface layers contribute to distortion within the overall pavement structure.

The magnitude of rut depth which could develop in the upper layers of a pavement structure (i.e., layer rutting) is related to the asphalt content, subgrade modulus, and time (or age). From this relationship it can be observed that "layer rutting" increases with time (or traffic), lower layer moduli, and lower asphalt contents.

## HMAC Overlay of HMAC

The equations for estimating rut depth development in flexible overlay sections are presented in Figure 14. Both equations have relatively high  $R^2$  values (i.e., 0.90 for "deep-seated" and 0.91 for "layer" rutting) and were developed from a total of ten SHRP LTPP sites. These equations should be considered preliminary and should be confirmed in future analyses.

From Figure 14, it can be observed that "deep-seated" rutting is a function of a number of variables including climate ( $C$ ), subgrade modulus ( $E_{SG}$ ), overlay layer modulus ( $E_{OL}$ ) and surface layer modulus ( $E_S$ ). "Deep-seated" rutting would apparently be greater for dry climates ( $C = -1$ ), lower subgrade moduli, and higher surface and overlay layer moduli.

On the other hand, the magnitude of "layer" rutting is influenced primarily by the modulus of the original surface layer with higher moduli values resulting in greater rutting depths.

## HMAC Overlay of PCC

The equation for estimating rut depth development in an HMAC overlay layer of a rigid pavement (Figure 15) is a function of subgrade type (i.e., fine or coarse grained), overlay layer thickness and moisture conditions. The equation has a reasonable  $R^2$  (0.68) and is based on the results from ten SHRP-LTPP sections. Because of the existence of the PCC layer, "deep-seated" rutting would not develop in this type pavement.

From Figure 15, it can be observed that the magnitude of rutting is expected to be greater for a coarse subgrade ( $SC = +1$ ), thicker overlays, and wetter environs ( $M = +1$ ).

## *Applications*

The equations presented in this document can be used in an initial pavement design selection process to identify those pavement structural sections which are prone to develop greater rutting depths and cross profile distortion.

The  $R_T$  equations (Figures 9, 10, and 11) could be used to identify the type of rutting (i.e., "layer" or "deep-seated") which could be expected to develop within the proposed design

## Results

### HMAC Overlay of HMAC

Deep  $\mathbf{RD = 3.6 - 1.75(C) - 0.06(E_{SG} - 31) - 0.001(E_{OL} - 300) + 0.005(E_S - 750)}$

$C = \text{freeze } +1, \text{ nonfreeze } -1$

$E_{SG} = \text{Subgrade Modulus, ksi}$

$E_{OL} = \text{Original Layer Modulus, ksi}$

$E_S = \text{Overlay Layer Modulus, ksi}$

$R^2 = 0.90 \quad \text{RMSE} = 0.8 \quad 6 \text{ Sites}$

Layer  $\mathbf{RD = 7.4 + 0.005(E_S - 750)}$

$E_S = \text{Overlay Layer Modulus, ksi}$

$R^2 = 0.91 \quad \text{RMSE} = 0.4 \quad 4 \text{ Sites}$

Figure 14. Rut Depth Equations - HMAC Overlay of HMAC

## Results

### HMAC Overlay of PCC

$$RD = 1.0 + 4.1(S_G) + 6.8(T_{OL} - 2.2) + 6.8(M)$$

where

$S_G$  = Subgrade Type

Coarse +1

Fine -1

$T_{OL}$  = Overlay Thickness, inches

$M$  = Moisture Conditions

wet +1

dry -1

$$R^2 = 0.68$$

$$RMSE = 3.8$$

10 Sites

Figure 15. Rut Depth Equation - HMAC Overlay of PCC

section. Preliminary adjustments in the designs could then be made to minimize the potential of development of both layer and deep-seated rutting.

Once the rut type is established for the proposed design section, then the appropriate rut depth prediction equation (Figures 12, 13, 14, and 15) could be used estimate the expected magnitude of long-term rutting. At this point in the process, the design section specifically could be adjusted (i.e.,  $T_s$ , AC,  $E_s$ ,  $E_{OL}$ ) to minimize the predicted magnitude of rutting.

It should be understood that this proposed process is based on rutting only and that the possible development of other types of distress (e.g., fatigue) in the pavement structure should also be considered in developing final flexible pavement structural sections.

## **SHRP Data Analysis Contract: Brent Rauhut Engineering Inc. and ERES Consultants Inc. (P-020)**

### *Introduction*

The initial fullscale analysis of the SHRP-LTPP data was completed by Brent Rauhut Engineering Inc. (BRE) and ERES Consultants Inc. (ERES). BRE pursued a flexible pavement analyses, while ERES conducted a rigid pavement analyses. SHRP's objectives for this research effort were to (1) develop and implement a strategic approach to the analysis of LTPP data that would support the overall goals of SHRP and LTPP and (2) to develop data analysis plans that could be followed in future analyses with LTPP data. The results of this study are included in five volumes (20, 21, 22, 23, 24).

To accomplish these objectives, the following activities were undertaken:

1. Data were received and/or extracted from the National Pavement Performance Database (NPPDB), processed, and assigned to databases for analysis. Statistical evaluations of these databases were conducted.
2. LTPP data were used to evaluate basic AASHTO design equations, and the possibility of developing improved design equations was investigated.
3. Sensitivity analyses were conducted to identify independent variables with significant effects on pavement performance and to quantify the relative effects of each.
4. Results of these early data analyses were used to recommend future data analysis requirements and approaches and knowledge of LTPP data.

Several databases were formed, each representing a combination of distress type and pavement type. Statistical evaluations of the separate databases provided characterizations of the data in the databases and identified shortcomings in the data.

It should be noted, however, that the quantity and quality of the data used in this study was less than desired. In some instances, data had to be generated or formulated to overcome missing or incomplete data.

## *Limitations Resulting from Data Shortcomings*

This project involved the analysis of data observed on in-service pavements, and the early data analysis results can only be as good as the quality of the database from which they are conducted. There are limitations in these studies that are an unavoidable consequence of the timing of the early data analyses. Data was analyzed which had not been exposed to the comprehensive quality assurance, quality control checks at either the regional information management system (RIMS) or the national information management system (NIMS). For instance, excellent traffic data acquired by the monitoring equipment recently installed will be available for future data analysts; however, this early data analysis was based on estimates of historical ESALs of questionable accuracy.

While years of time-sequence monitored data will eventually be available, these studies included distress measurements for only one point in time, or at most two. For most distresses, an additional data point could be inferred for conditions immediately after construction (e.g., rutting, cracking, and faulting of joints may generally be taken as zero initially). However, for most test sections, analyses of pavement roughness increases depended on educated estimates of initial roughness which were derived from SHA estimates of initial PSI. Similarly, the evaluations of the basic AASHTO design equations depended on the SHA estimates of initial pavement PSI.

Another shortcoming of this study, which no doubt, impacted the results was the unavailability of some inventory data elements, particularly the data from SHA project files concerning the design and construction of the pavements. Some data elements were available for all the test sections, while other data elements were unknown and unavailable for some test sections. Unfortunately, it will not be possible to acquire much of the missing inventory data, which will be missing for future analyses as well.

The number of LTPP sections which exhibited distress was limited and those with distresses would generally exhibit only one or two types. The distress type that was generally available for all test sections was pavement roughness within the SHRP-LTPP time frame. In this instance, however, it was necessary to estimate the initial roughness to define increases in roughness. Rutting information was available for nearly all flexible pavement test sections. On the other hand it was not possible to study alligator cracking in flexible pavements since only 18 test sections were reported to have any alligator cracking. Raveling and weathering distress was limited to three sections and could not be evaluated. The flexible pavement distress types for which sufficient data were available to support this study included rutting, change in roughness (measured as IRI), and transverse (or thermal) cracking.

It became apparent early in this analysis that satisfactory global predictive flexible pavement (HMAC) models could not be developed from all the data in the NPPDB because of the size of the inference space and environmental zones, which included all of the United States and parts of Canada. Consequently, when sufficient test sections were available that displayed the particular distress type, regional databases were formed for each of the four environmental regions and separate regional HMAC predictive models were developed. This regionalization

was not possible for the rigid (PCC) pavements because the resulting regional databases would include too few data.

Predictive models for PCC pavements could be developed for ten combinations of pavement type and distress type. The models included joint faulting for doweled and non-doweled joints, transverse cracking for jointed plain concrete pavement (JPCP), transverse crack deterioration for jointed reinforced concrete pavement (JRCP), joint spalling for JPCP and JRCP, and IRI for doweled JPCP, non-doweled JPCP, JRCP, and continuously reinforced concrete pavement (CRCP). Insufficient data were available to develop regional predictive models.

The study of overlaid pavements was to have been of high priority in SHRP-LTPP. It was decided early in the implementation of the SHRP-LTPP studies that pavement test sections would be sought for which overlays were imminent, so that the condition before overlay would be available. Pavement condition before overlay was considered a critically important variable; however, this information was not available for pavements that were overlaid before acceptance in the GPS. Several test sections have been overlaid, but none are old enough to have appreciable distress. In this study, the total numbers of overlaid pavements were limited, and few had sufficient information for successful analyses. Consequently, analyses for the overlaid pavements were limited to an evaluation of the 1993 AASHTO Overlay Design Equations.

## **Sensitivity Analyses and Results**

"Sensitivity analysis" is not a common term to either research engineers or statisticians, but it has come to have a specific meaning to some advocates from both disciplines. In this research effort, sensitivity analyses were defined as statistical studies to determine the sensitivity of a dependent variable to variations in independent variables (sometimes called explanatory variables) over reasonable ranges.

There is no single accepted method of conducting sensitivity analyses; however, all approaches require the development of an adequate equation (or model) as a beginning point. The approach used in these studies involved setting all explanatory or independent variables in a predictive equation at their mean levels and then varied them individually, one at a time from one standard deviation above to one standard deviation below the mean variable level. The relative sensitivity of the distress prediction for a particular variable is defined as the change in the predicted distress across the range of two standard deviations of explanatory variable. These changes in predicted stresses are compared with distress changes when the other explanatory variables are varied in the same manner.

An example of a sensitivity analysis is presented in Table 22 for the rutting predictive equation for a wet-freeze environmental zone. The form of the equation is presented at the top of the table, and the explanatory variables or interactions are included in the table, along with the coefficients that provide the details of the equation. The exponents *B* and *C* are calculated by multiplying the explanatory variables or interactions in the left column by the

Table 22. Coefficients of Regression Equations Developed to Predict Rutting in HMAC on Granular Base for the Wet-Freeze Dataset

$$\text{Rut Depth} = N^B 10^C$$

where

$N$  = number of cumulative KESALs

$B = b_1 + b_2 x_1 + b_3 x_2 + \dots + b_n x_{n-1}$

$C = c_1 + c_2 x_1 + c_3 x_2 + \dots + c_n x_{n-1}$

Explanatory Variable ( $x_i$ )	Units	Coefficients for Terms In	
		$b_i$	$c_i$
Constant Term	--	0.183	0.0289
log(Air Voids in HMAC)	% by volume	0	-0.189
log(HMAC Thickness)	In.	0	-0.181
log(HMAC Aggregate < #4 Sieve)	% by weight	0	-0.592
Asphalt Viscosity at 140°F	Poise	0	$1.80 \times 10^{-5}$
log(Base Thickness)	In.	0	-0.0436
Annual Precipitation	In.	0	
Freeze Index	Degree-days	0	$3.23 \times 10^{-6}$

$n$  = 41  
 $R^2$  = 0.73  
 Adjusted  $R^2$  = 0.68  
 RMSE in  $\log_{10}$ (Rut Depth) = 0.19

regression coefficients  $b_i$  and  $c_i$  and adding the results. For example, the constant  $b_1$  for this model is 0.183 and is equal to  $B$  because all the other  $b_i$ 's are 0. To calculate  $C$ , the constant term is 0.0289, the log of air voids in HMAC is multiplied by -0.189, and so forth.

The results of the sensitivity analyses conducted with this predictive equation appear as Figure 16. From Figure 16, it can be seen that the greatest effect on the occurrence of rutting in the wet-freeze environment may be expected to be the number of KESALs. The dashed lines to the left indicate that reductions in KESALs decrease rutting; however, it should be recognized in this case that the standard deviation for KESALs is greater than the mean, and negative KESALs are not possible. Freeze index is the next most important, followed by percent of the HMAC aggregate passing a #4 sieve, air voids, and so forth. It can also be seen from the directions of the arrows that increasing KESALs and freeze index may be expected to increase rut depths, while increasing amounts of aggregate passing the #4 sieve, air voids, and asphalt thickness may be expected to decrease rutting.

To illustrate how the sensitivities may differ from one environmental region to another, the sensitivity analysis results for the dry-nonfreeze environmental zone are included as Figure 17. In comparing the results of the two datasets, it can be seen that the majority of the variables are the same but that there are some differences and that the relative levels of sensitivities vary between environmental zones.

Similar studies were conducted for rutting in other environmental regions, as well as for increases in roughness and transverse crack spacing in all four environmental regions. For PCC pavements, global equations to predict the occurrence of distresses were developed using the entire databases, and sensitivity analyses were carried out in the same manner.

While the sensitivity analyses offer useful insight, it must be remembered that most of these pavements are in very good shape, so some important interactive effects---such as water seeping through cracks and expediting deterioration in lower layers---are not necessarily represented in these results.

### *Summary of Sensitivity Analysis Results for HMAC Pavements*

The twelve significant variables from the sensitivity analyses for HMAC pavements are listed in Table 23 by distress type, by relative ranking, with the most significant variable at the top and the least significant at the bottom.

Nine variables were significant in all three distress types. The exceptions are listed below:

- Air-void level in HMAC was not significant for transverse cracking
- Percentage of HMAC aggregate passing a #4 sieve was not significant for change in roughness

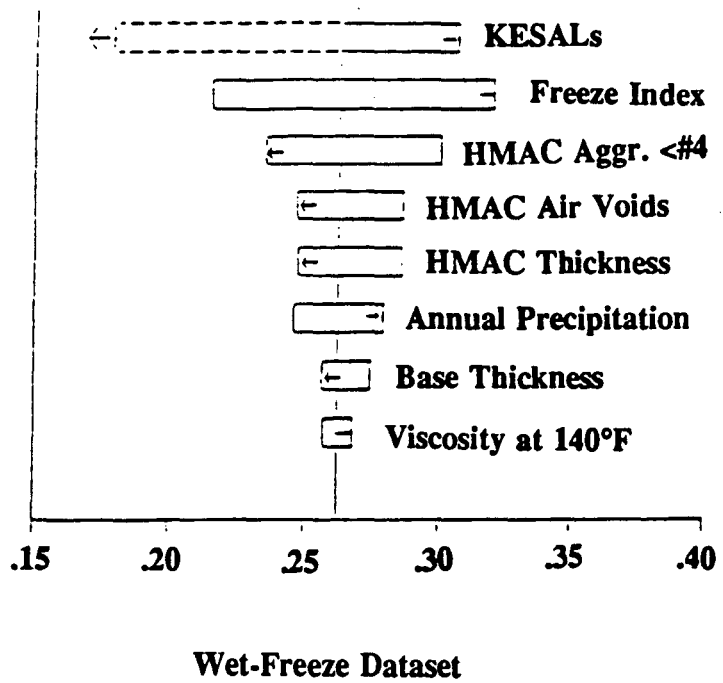


Figure 16. Results of Sensitivity Analysis for Rutting in HMAC Granular Base

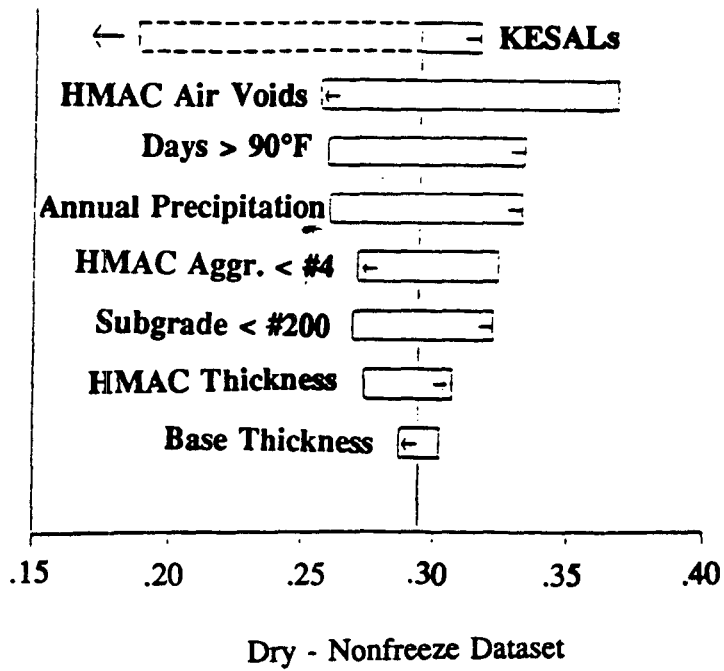


Figure 17. Results of Sensitivity Analysis for Rutting in HMAC on Granular Base

**Table 23. Sensitivity Analysis Results: HMAC**

<b>Rutting</b>	<b>Change in Roughness</b>	<b>Transverse Cracking</b>
KESALs Air Voids in HMAC HMAC Thickness Base Thickness Subgrade < #200 Sieve Days with Temp. > 90°F HMAC Aggregate < #4 Sieve Asphalt Viscosity Annual Precipitation Freeze Index Base Compaction Average Annual Min. Temp.	KESALs Asphalt Viscosity Days with Temp. > 90°F HMAC Thickness Base Thickness Freeze Index Subgrade < #200 Sieve Air Voids in HMAC Base Compaction Annual Precipitation Daily Temp. Range Annual Freeze-Thaw	Age Annual Precip. HMAC Thickness Base Thickness Asphalt Viscosity Base Compaction Freeze Index Days with Temp. > 90°F Subgrade < #200 Sieve KESALs Annual Freeze-Thaw Cycles HMAC Agg. < #4 Sieve Cycles

- Annual number of freeze-thaw cycles was not significant for rutting
- Average annual minimum temperature and daily temperature range were significant only for rutting and change in roughness, respectively

In addition, four environmental variables were found to be significant for rutting, five for change in roughness, and four for transverse cracking.

Some recommendations and comments associated with the sensitivity analyses follow:

1. Most of the rutting for these pavements apparently occurred soon after they were opened to traffic. These pavements do not necessarily represent the case of advanced deterioration.
2. It is important to achieve sufficient compaction so that the early compaction under traffic is not excessive.
3. The amount of HMAC aggregate passing the #4 sieve was selected to represent the effects of gradation. Within the inference spaces of the separate datasets, increasing amounts of aggregate passing the #4 sieve appeared to reduce rutting.
4. As expected, traffic loading was the strongest contributor to rutting and roughness, while pavement age had the strongest effect on transverse cracking.
5. Thicker HMAC surface layers and the use of granular base layers may be expected to decrease all three types of distress.

Some of these results are difficult to explain. For example, the studies indicate that increases in base compaction, annual precipitation, asphalt viscosity, or annual freeze-thaw cycles (or freeze index) tend to increase transverse crack spacing (reduce cracking). These results are difficult to understand and cannot be explained entirely in terms of reliabilities of the equations, since the regional equations had fairly good statistics. This could be indicative of a significant interaction effect which was not fully developed within the regional data.

In summary, most of the results from the sensitivity analyses for HMAC pavements appear to be reasonable; however, other results appear as surprises that may (1) result from the specific characteristics of the datasets on which they are based, (2) represent mechanisms not yet understood, (3) result from interactions not explained by the equation forms, or (4) result from other unknown causes.

### *Summary of Sensitivity Analysis Results for PCC Pavements*

The results of the sensitivity analyses on PCC pavements are presented in Table 24. The independent variables are listed below in order of "combined rankings," one based on average

**Table 24. Sensitivity Analysis Results: PCC**

<b>Ranking by Average</b>	<b>Ranking by Number of Models Found Significant</b>
Age Cumulative ESALs Slab Thickness Static <i>k</i> Value Precipitation Joint Spacing Percent Steel Edge Support (Tied Shoulders) Annual Freeze-Thaw Cycles Type of Subgrade PCC Flexural Strength Monthly Temperature Range Widened Traffic Lane Freeze Index Dowel Diameter Subdrainage Type of Base	Age Cumulative ESALs Slab Thickness Static <i>k</i> Value Precipitation Edge Support (Tied Shoulders) Joint Spacing Percent Steel Annual Freeze-Thaw Cycles Type of Subgrade PCC Flexural Strength Monthly Temperature Range Widened Traffic Lane Freeze Index Dowel Diameter Subdrainage Type of Base

rankings and one based on number of models in which the variable was included. In case of a tie, the other ranking basis was used to order the two.

The rankings are almost identical for the two methods. However, the results in Table 24 do not tell the whole story, since the rankings depend on type of pavement and type of distress. Conclusions concerning the three PCC pavement types (JPCP, JRCP, and CRCP) have been developed from the results of the sensitivity analysis and past experience. The conclusions are presented in the following sections.

### Design Recommendations for Jointed Plain Concrete Pavement (JPCP)

1. Use of dowels of sufficient size for the traffic loadings (the larger the dowel diameter, the less faulting) will ensure that faulting will not become significant and cause severe roughness. Use of dowels is particularly important for heavy traffic in cold and wet climates. Thicker slabs by themselves do not reduce faulting significantly. Longitudinal subdrainage will help reduce faulting of non-doweled joints. Use of a tied concrete shoulder will reduce doweled joint faulting.
2. Increased slab thickness has a very strong effect on reducing transverse slab cracking and providing a smoother JPCP (lower IRI) over time.
3. Provision of increased subgrade support, as indicated by the back-calculated  $k$  value, results in lower IRI and a smoother pavement. Increased support over an existing soft subgrade would likely require either treatment of the soil or a thick granular layer over the subgrade.
4. Use of shorter slabs for JPCP will reduce the amount of joint faulting and transverse cracking and will result in a smoother pavement (lower IRI) over time.
5. Specification of durable concrete in freeze climates is desirable, so that freeze-thaw cycles and other climatic factors do not result in significant joint spalling.

### Design Recommendations for Jointed Reinforced Concrete Pavement (JRCP)

1. Use of dowels of sufficient size for the traffic loadings (the larger the dowel diameter, the less faulting) will ensure that faulting will not become significant and cause severe roughness. Use of dowels is particularly important for heavy traffic in cold and wet climates. Thicker slabs by themselves do not reduce faulting significantly. Longitudinal subdrainage will help reduce faulting of non-doweled joints. Use of a tied concrete shoulder will reduce doweled joint faulting.
2. Increased slab thickness has a very strong effect on reducing transverse slab cracking and providing a smoother JRCP (lower IRI) over time.

3. Provision of increased subgrade support, as indicated by the back-calculated  $k$  value, results in lower IRI and a smoother pavement. Increased support over an existing soft subgrade would likely require either treatment of the soil or a thick granular layer over the subgrade.
4. Use of shorter JRCP slabs will reduce the amount of joint faulting.

### Design Recommendations for Continuously Reinforced Concrete Pavement (CRCP)

1. Increased percentage of longitudinal reinforcement provides a smoother CRCP (lower IRI) over time. The increased percentage of steel reduces the number of punchouts and the deterioration of transverse cracks.
2. Increased subgrade support results in fewer deteriorated transverse cracks and a lower IRI (smoother pavement). Increased support over an existing soft subgrade would likely require either treatment of the soil or placement of a thick granular layer over the subgrade.
3. Widened traffic lanes will provide a smoother CRCP (lower IRI) over time.
4. Increased slab thickness results in somewhat smoother CRCP (lower IRI) over time, probably because there are fewer punchouts as a result of the thicker slab.

### *Evaluation of the AASHTO Flexible Pavement Design Equation*

The equation, which was evaluated in this study, is the one included in the 1986 *AASHTO Guide for Design of Pavements*:

$$\log W = Z_R * S_o + (G/\beta) + 2.32 \log M_r - 8.07$$

where

- $G_i = \beta (\log W - \log \rho) = \log (\Delta\text{PSI}/2.7)$   
 $W =$  number of 18-kip ESALs  
 $\rho = 0.64 (\text{SN} + 1)^{9.36}$   
 $\beta = 0.4 + 1094/(\text{SN} + 1)^{5.19}$   
 $\text{SN} = a_1 D_1 + a_2 m_2 D_2 + a_3 m_3 D_3 + \dots + a_n m_n D_n$   
 $D_i =$  thickness of Layer  $i$  (in.)  
 $a_i =$  structural coefficient for the material in Layer  $i$   
 $m_i =$  drainage coefficient for the material in Layer  $i$   
 $Z_R =$  standard normal deviate  
 $S_o =$  overall standard deviation  
 $M_r =$  resilient modulus (psi)

Because this equation was used for research instead of design, a 50% reliability was assumed, which resulted in  $Z_R = 0$ .

The original equation for calculating current PSI was reported in the *AASHTO Road Test Report 5* as follows:

$$\text{PSI} = 5.03 - 1.91 \log(1 + sv) - 1.38rd^2 - 0.01 \sqrt{c + p}$$

where

sv = average slope variance as collected using the CHLOE profilograph

rd = average rut depth based on a 4-ft straightedge

c = Class 2 and Class 3 cracking (ft<sup>2</sup> per 1000 ft<sup>2</sup>)

p = bituminous patching (ft<sup>2</sup> per 1000 ft<sup>2</sup>)

This equation, commonly used in the past for estimating PSI, was used to determine current PSI values for the SHRP-LTPP sections from values of slope variance derived from surface profiles measured with a Law profilometer and rut depths measured by PASCO's RoadRecon unit. The cracking and patching terms were not included in the calculation of the current PSI, since significant cracking and patching (c&p) were only noted for a few test sections. In addition, the effect of the c&p term was not considered significant because with a coefficient of 0.01, a significant amount of cracking patching would be required to influence the PSI estimate. The mean value of current PSI for the SHRP-LTPP sections included in this analysis was 3.53, with a standard deviation of 0.49.

Observed PSI loss was defined as the difference between an initial estimated PSI value and the calculated current PSI value. The mean value for observed PSI loss was 0.70 and the standard deviation was 0.51. Initial values of PSI were estimated by the SHAs, resulting in a mean value of 4.25 and a standard deviation of 0.23.

The basic AASHTO equation was used to predict the total KESALs required to cause the observed losses in PSI. Rearranging the equation slightly results in

$$\Delta\text{PSI} = 2.7 (W/pS_m)^{\beta}$$

where

$$S_m = (M_r)^{2.32} * 10^{-8.07}$$

The predicted PSI losses associated with the historical traffic estimated by the SHAs were calculated with this equation.

Resilient moduli estimates for the subgrade ( $M_r$ ) were obtained from the back-calculation procedures recommended in the 1986 *Guide*, using the deflections measured by an outer sensor of an FWD. Historical traffic data provided by the SHAs were used for the traffic data ( $W$ ) in these calculations. The cumulative KESALs for each section were divided by the

number of years since the test section was opened to traffic to obtain average values per year. This allowed extrapolation to an extra year or two beyond 1989 to obtain traffic level estimates associated with the dates of monitoring activities. Most of the monitoring data used were obtained in 1990 or 1991.

During the investigation it was found that the roughness based KESAL estimates were consistently much higher than the historical estimates of the SHAs. Only 9 of the 244 predictions were lower than the SHA estimates, while the predictions were more than 100 times the SHA estimates for 112 test sections. As the predictions from the design equation appeared to be very poor for in-service pavements, the thrust of the research turned toward identifying its problems and developing more reliable equations.

As partial explanation, it was noted that 74% of the in-service test sections in this study had experienced a loss in PSI of 1.0 or less, while those in the road test experienced losses of 2 to 3. Further, the average absolute deviation of observed PSI from the computed curves at the AASHTO Road Test was 0.46, so some 39% of the in-service test sections in this study had experienced losses of PSI within the "noise" at the road test.

Linear regressions conducted on the database resulted in an equation with an  $R^2$  of 0.09, indicating that the equation form simply did not represent in-service pavement performance. Additional factorial studies indicated that the equation appears to falter for structural numbers less than 3, cumulative traffic greater than 5 million ESALs, or subgrade moduli greater than 10,000 psi (a value of 3000 psi was assumed for the road test data)---that is, for conditions outside the inference space of the AASHTO Road Test.

Linear regression analyses were conducted to correlate the ratio of predicted to observed traffic within structural number, subgrade modulus, PSI loss, average annual rainfall and average number of days below freezing. This analysis resulted in an equation with a coefficient of determinations,  $R^2$  of 0.77.

In a review of subgrade moduli back-calculation from falling weight deflectometer (FWD) results, the values resilient moduli laboratory testing was just getting underway when these analyses were being conducted. Subsequent comparisons of 106 test sections for which laboratory  $M_r$  results were available, it was found that the mean ratio of back-calculated to laboratory-derived moduli was 4.48, with a standard deviation of 2.47 when these 106 laboratory moduli were substituted for the back-calculated moduli, the ratios of predicted to observed ESALs were considerably decreased. The number of "reasonable predictions" (with ratios of 2 or less) changed from 13 with the back-calculated subgrade moduli to 60 with the laboratory moduli. While the predictions improved greatly, the ratios for 46 predictions still ranged from 2 to more than 100. It appears certain that future design equations must take into account differences between back-calculated and laboratory-derived resilient moduli.

Other limitations of the flexible pavement design equation were noted:

1. The accelerated trafficking to "failure" at the road test was not necessarily representative of in-service pavements. Pavement engineers typically intercede with overlays or other

rehabilitation long before serviceability loss approaches the level normally considered as terminal at the road test.

2. The subgrade elastic moduli were assumed to be 3000 psi for the test sections at the AASHTO Road Test in the development of equations at the road test. Much higher moduli results were observed from either back-calculation of FWD results or from current  $M_r$  laboratory testing.

### *Evaluation of the AASHTO Rigid Pavement Design Equation*

This investigation was undertaken using the original AASHTO design equation and the 1986 extension of the original design equation, which was unchanged in the 1993 guide. The analysis using the AASHTO original equation was undertaken to determine whether the improvements to the prediction model were beneficial.

The AASHTO design equations were evaluated by comparing the predicted 18-kip (80-kN) ESALs for each test section determined from the design equation with the "observed" ESALs (estimated from historical traffic data) carried by the section. The predicted ESALs were calculated using the concrete pavement design equations from the original Road Test and the latest extended form included in the 1986 *AASHTO Design Guide for Pavement Structures*.

The original 1960 AASHTO design equation included the following relationship between serviceability loss, axle loads and types, and slab thickness:

$$G_t = \beta(\log W_t - \log p) = \log([4.5 - p_t] / [4.5 - 1.5])$$

where

- $G_t$  = logarithm of the ratio of loss in serviceability at time  $t$  to the potential loss taken to a point at which serviceability equals 1.5
- $\beta$  = a function of design and load variables that influence the shape of the  $p$ -versus- $W$  serviceability curve
- $W_t$  = cumulative 18-kip ESALs applied at end of time  $t$
- $p$  = a function of design and load variables that denotes the expected number of axle load applications to a terminal serviceability index
- $\log p = 7.35 \log(D + 1) - 0.06$
- $D$  = slab thickness (in.)
- 4.5 = mean initial serviceability value of all sections
- $p_t$  = terminal serviceability

In both the 1986 and 1993 *AASHTO Design Guides*, the PCC pavement design model is given as:

$$\log W_{18} = Z_R S_o + 7.35 \log(D + 1) - 0.06 + \frac{\log\left(\frac{\Delta PSI}{4.5 - 1.5}\right)}{1 + \frac{1.624 * 10^6}{(D + 1)^7}}$$

$$+ (4.22 - 0.32\rho) \log\left(\frac{S'_c C_d (D^{0.75} - 1.132)}{215.63 J [D^{0.75} - \frac{18.42}{(E_c/k)^{0.25}}]}\right)$$

where

- $\Delta PSI$  = loss of serviceability ( $p_i - p_f$ )
- $D$  = thickness of PCC pavement (in.)
- $S'_c$  = modulus of rupture of concrete (psi)
- $C_d$  = drainage coefficient
- $E_c$  = elastic modulus of concrete (psi)
- $k$  = modulus of subgrade reaction (psi/in.)
- $J$  = joint load transfer coefficient
- $W_{18}$  = cumulative 18 kip ESALs at end of time  $t$
- $p_i$  = initial serviceability
- $p_f$  = terminal serviceability
- $Z_R$  = standard normal deviate
- $S_o$  = overall standard deviation

Five sets of analyses were performed for each GPS-3 (JPCP), -4 (JRCP), and -5 (CRCP) to examine the capability of the equations to predict the amount of traffic actually sustained by each test section. Analyses were conducted initially on all data available for each of the three experiments. The datasets for each pavement type (JPCP, JRCP, and CRCP) were further separated into environmental regions and analyses for each of the pavement types were then performed for each of the four environmental regions.

The predicted KESALs obtained from the AASHTO equation were plotted against the estimated KESALs from historical data on scattergrams to visually examine the scatter of the data. The plot of predicted KESALs versus historical KESALs obtained from the original AASHTO model appears in Figure 18 for JPCP and JRCP. If the predictions were unbiased for all regions, half the points would fall on each side of the line of equality. It can be seen that the original AASHTO model over predicts KESALs for a majority of test sections (78% of JPCP and 82% of JRCP). Similar scatterplots were developed for separate environmental regions.

The plots of predicted KESALs obtained from the 1986 or 1993 AASHTO model versus historical KESAL estimates for JPCP are shown in Figure 19. It can be seen that the 1993 model predicted KESALs much better than the original AASHTO model for these analysis datasets, suggesting that the addition of several design factors considerably improved the performance prediction of the model. However, there is still scatter about the lines of

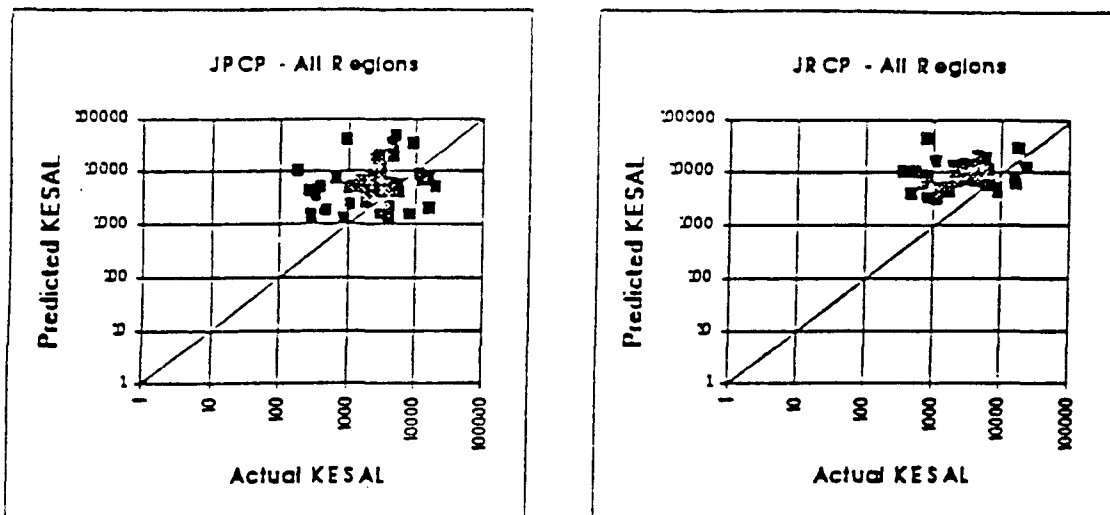


Figure 18 Predicted KESALs versus Actual KESALs for JPCP and PRCP Using Original AASHTO Prediction Models

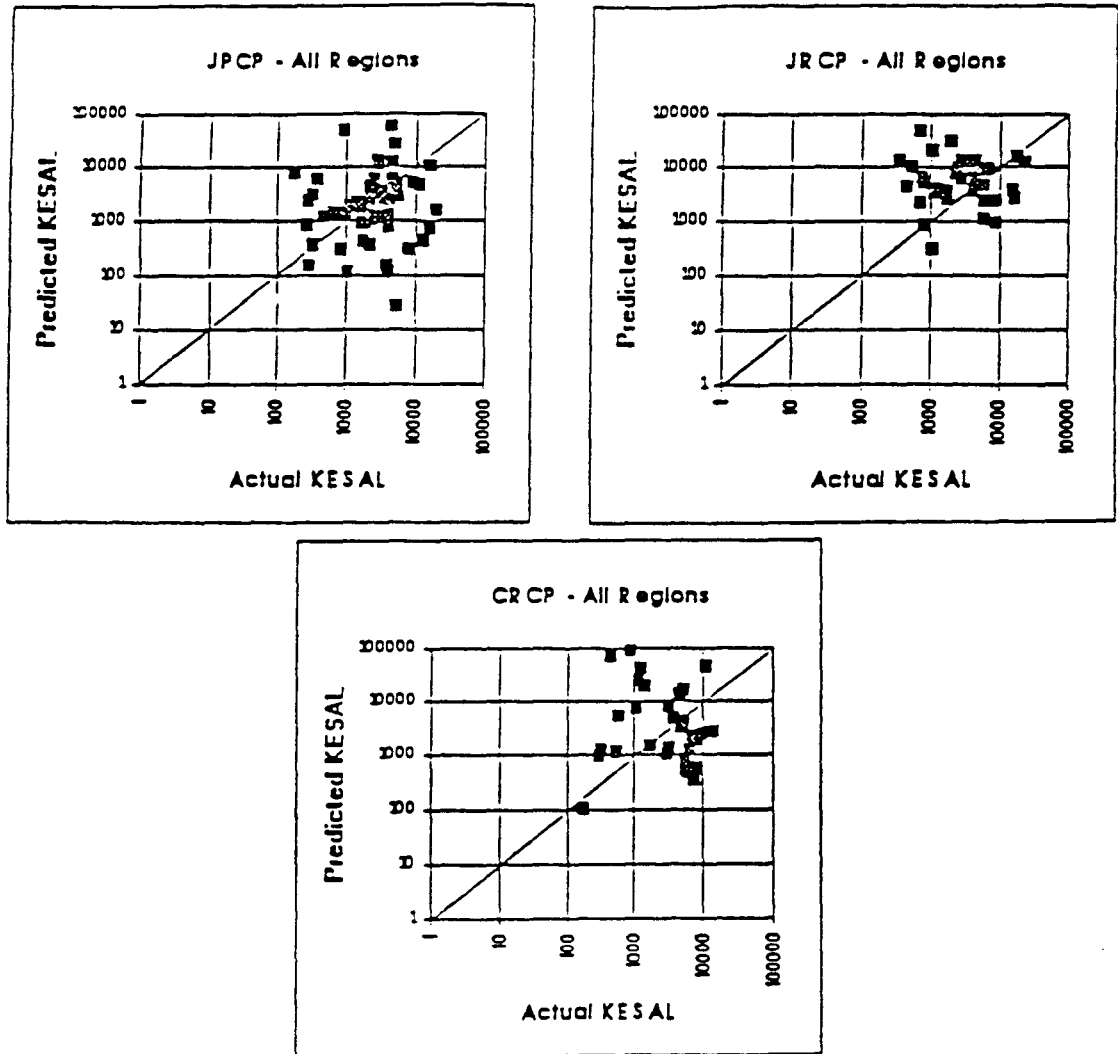


Figure 19 Predicted KESALs versus Actual KESALs for JPCP, JRCP, and CRCP Using 1993 AASHTO Prediction Models

equality, even on these log-log plots. This scatter may be due to several causes, including inadequacies in the model, errors in the inputs, and random performance variations (or pure error). Similar plots were prepared and evaluated for JPCP and CRCP.

In order to analytically assess the capability of the AASHTO concrete pavement design model to predict the actual historical KESALs for the pavement sections, a statistical procedure was selected that can be used to determine whether two sample datasets (actual and predicted) are from the same population. The paired-difference method, using the Student  $t$  distribution, was used to determine whether the KESALs as predicted by the AASHTO equation statistically belong to the same population as the historically developed KESALs.

Appropriate statistical analysis tools were then used to compare the historical KESALs with those predicted by the AASHTO equations. The calculated  $t$  statistic ( $t$ -calc) was compared with a tabulated  $t$  statistic ( $t$  table) for a specific confidence level. If  $t$  calc was greater than  $t$ -table, the null hypothesis (that they are from the same population) is rejected with a 5% chance of error, since the confidence level selected for this analysis is 95%.

It was observed that  $t$ -calc was greater than  $t$ -table for half the datasets when the original AASHTO model was used, which indicates that the original AASHTO model may not be a reliable predictor of the historically generated ESALs for the pavement sections. On the other hand, the results for the 1993 AASHTO model indicate that the null hypothesis is not rejected. This result was found true for all climatic regions. The improvements to the original AASHO model undoubtedly increased the accuracy of the design equation.

Another comparative evaluation was made between the historical estimates KESALs and predicted KESALs at a particular level of design reliability. Thus, the mean log  $W_{50\%}$  prediction is reduced by  $Z_R S_o$  (where  $Z_R = 1.64$  for 95% reliability and  $S_o = 0.35$ ). The predicted (at 95% reliability) versus the historical KESALs were plotted. Most of the points plotted below the line of equality, indicating that the consideration of design reliability definitely results in a large proportion of sections (77%) with a conservative design, a desirable result.

The results of these studies indicated that the 1986 (or 1993) model appears to provide more or less unbiased predictions in that the plots of predicted versus historical KESALs tend to center on the lines of equality. Although the scatter is not very apparent on the log-log plots, which was used to insure the inclusion of all the data points, the actual scatter is obvious when reviewed arithmetically. Collectively, the adjustments to the 1993 model seems to have improved the predictive capabilities over the original AASHTO model. This evaluation points out the need for continued model improvements to increase the accuracy of the predictions.

### *Evaluation of the 1993 AASHTO Overlay Design Equations*

The 1993 revisions to the AASHTO overlay design procedure were instituted to provide overlay thicknesses that address a pavement with a structural deficiency. A structural deficiency can arise from any condition that impairs the load-carrying capability of the

pavement structure. These conditions could include inadequate thickness, cracking, distortion, and disintegration.

The AASHTO pavement overlay design procedures are based on the concept that time and traffic loading reduce a pavement's ability to carry loads. An overlay is designed to increase the pavement's ability to carry loads over a future design period. The structural capacity required for a PCC or HMAC pavement to carry future traffic can be calculated with the appropriate AASHTO 1993 pavement design equation. The effective structural capacity of the existing pavement is assessed using procedures for overlay design presented in the *Guide*. These procedures can be based on visual survey and materials testing results, on the remaining life of the pavement in terms of the traffic that can be carried, or on nondestructive testing (NDT) of the existing pavement. An overlay is then designed on the basis of the structural deficiency represented by the difference between the structural capacity required for future traffic and the effective structural capacity of the existing pavement.

The results and data from LTPP GPS-6A, GPS-6B, GPS-7A, GPS-7B, and GPS-9 experiments were used to evaluate the viability of the 1993 version of the AASHTO overlay design equations. While data on design life and levels of reliability sought were unavailable, a limited set of test sections was identified that had sufficient data for limited evaluations. The set included nine sections with HMAC overlays of HMAC, five with HMAC overlays of PCC, and six with unbonded PCC overlays of PCC. Even for these test sections, it was necessary to use existing data to estimate values for some of the inputs for the design equations.

The design equations were used to predict required overlay thicknesses, and these thicknesses were compared with the actual thicknesses of the overlays. The results from recent profile measurements and distress surveys were also used to evaluate the adequacy of the AASHTO design equation for establishing an appropriate design overlay thickness. Table 25 is a summary of the results from these comparative evaluations.

Although these evaluations were seriously constrained by data limitations in this small dataset of five test sections the equation appears to work quite well for AC overlays of PCC. However, the evaluations were generally inconclusive for AC overlays of AC and unbonded PCC overlays of PCC. Further evaluations are needed for these pavement overlay types.

It is hoped that in future data on design periods and levels of reliability appropriate to design of overlays will be sufficient to sustain appropriate comparative evaluations.

### *Recommendations for Future Analyses*

One of the primary objectives of this research effort was the development of recommendations for future analyses particularly when more time series data will be available.

Table 25. Results from Comparative Evaluation of 1993 AASHO Overlay Equations

Test Section Number	Type of Pavement	Results From Comparisons			
		Conservative	Adequate	Inadequate	Inconclusive
016012	AC/AC		X		
016109	"				X
351002	"				X
356033	"				X
356401	"		X		
486079	"		@95%		
486086	"		Reliability		X
486160	"	X			
486179	"				X
Subtotals for AC/AC:		1	3	0	5
087035	AC/PCC		X		
175453	"		X		
283097	"		X		
287012	"		X		
467049	"			X	
Subtotals for AC/PCC:		0	4	1	0
69049	PCC/PCC			X	
89019	"				X
89020	"				X
269029	"				X
269030	"				X
489167	"				X
Subtotals for PCC/PCC:		0	0	1	5
Overall subtotals:		1	7	2	10

Future analytical objectives should include (1) development of distress models for use in design procedures, pavement management, and sensitivity analyses; (2) calibration of existing mechanistic-empirical models using LTPP data; (3) combining knowledge from SHRP studies of asphalt, concrete, and long-term performance to improve performance models and gain additional insight into effects of independent variables on performance; (4) development of models for layer stiffnesses in terms of component characteristics; and (5) evaluation of seasonal changes in layer stiffnesses and surface profiles.

Several modeling techniques for future analyses, were suggested by various experts each with its own set of strengths and weaknesses. Techniques that should be considered during future analyses include (1) those developed for these early analyses, (2) discriminate analysis, (3) techniques using "censored data" (World Bank procedures used in the Brazil Study and others), (4) survival analysis, (5) neural network approaches (relatively new applications to engineering systems), and (6) other nonlinear models.

### **SHRP Data Analysis Contract: Michigan State University (P-020B)**

This study represents an initial mechanistic evaluation of the AASHTO design procedures using the data from the SHRP database relative to the asphalt-surfaced GPS sections. The results of the mechanistic analysis were originally intended to accomplish the following objectives:

1. Calibrate the AASHTO design equations
2. Verify and calibrate the concept of the AASHTO drainage coefficient
3. Revise the AASHTO LEFs
4. Develop mechanistic-empirical models

Because some of the data elements required for the mechanistic analysis were incomplete and missing (e.g., resilient modulus data was not yet available) the research plan was modified to include the following tasks:

1. Establish a full-factorial experiment design matrix of 243 artificial flexible pavement sections. For each section, assign material properties and traffic volumes (in terms of 18-kip ESAL) within the typical ranges used by various SHAs. Design each pavement section (i.e., determine the required layer thicknesses) by the AASHTO design procedure. The layer thicknesses and the materials properties were then used to calculate the mechanistic responses (stresses, strains, and deflections) of each pavement section.
2. Conduct a sensitivity analysis of the mechanistic responses to the layer thicknesses established by the AASHTO procedure. Evaluate and revise as possible the AASHTO design equation and the concept of drainage coefficients.

## *Premises of the AASHTO Design Procedure for Flexible Pavements*

The principal premises associated with the AASHTO flexible pavement design are enumerated below:

1. An important variable of the AASHTO flexible pavement design equation is the structural number (SN) of the pavement. The SN is influenced by the traffic volume (in terms of 18-kip ESAL), design reliability, overall standard deviation, total loss of serviceability during the performance period, and resilient modulus of the roadbed soil. A pavement structural number is selected which will assure the structural capacity required to carry the anticipated traffic load and volume, yet only experience the specified loss of serviceability during the performance period. Hence, for any pavement structure, the AASHTO structural number is seemingly independent of the quality and properties of the asphalt, base, and subbase layers. The properties of these layers (e.g., layer coefficients) play a major role in establishing the thickness of each layer but not the overall pavement structural capacity in terms of the SN.
2. After determining the required SN of a pavement section, the layer thicknesses are computed by the recommended AASHTO layer analysis method. The AASHTO method assumes that an assigned structural capacity of the pavement is the sum of the structural capacity of each of its layers. Further, the SN of any pavement layer is the product of a material type coefficient, drainage coefficients and its thickness. Thus, the structural capacity of a relatively weak pavement layer (i.e., low material coefficient) can apparently be enhanced by increasing its thickness.
3. Although the AASHTO design guide advocates the use of good-quality materials with reasonable costs, the AASHTO procedure assumes that the effects of poor drainage on pavement performance can be ameliorated by adjusting the thickness of the affected layer. That is, a base layer with an excellent drainage quality would perform exactly the same as one with poor drainage quality, as long as the thickness of the layer is increased by the inverse of the ratio of the values of their drainage coefficients.
4. The effects of serviceability loss due to environmental conditions (freeze-thaw and swelling soils) can be ameliorated by increasing the structural capacity (SN) of the pavement. Higher environmental loss of serviceability requires higher structural capacity.

## *Mechanistic Evaluation/Calibration of the AASHTO Design Procedure*

After the 243 conceptual pavement sections were designed and the thicknesses of the various pavement layers established by the AASHTO design procedure, the mechanistic responses (stresses, strains, and deflections) were computed for of each pavement section using the linear option of the MICHPAVE computer program (a linear/nonlinear finite element program). The findings of the sensitivity analyses of the mechanistic outputs and results of comparison with the premises of the AASHTO design procedure are presented below:

1. For pavement sections with various layer properties yet designed by the AASHTO procedure for the same roadbed soil, traffic volume, and serviceability loss during an equal performance period, the mechanistic analyses indicate that:
  - a) The peak pavement surface deflection (a mechanistic response) is almost the same for all sections. Hence the amount of the overall damage due to compression into the various pavement sections (or the overall protection level) is constant and independent of the layer properties. This finding implies that the AASHTO design procedure produces a balanced design relative to the global damage delivered to the pavements. Stated differently, the results of the mechanistic analyses tend to support the structure and validity of the SN concept of the original AASHTO design equation.
  - b) Under loading, stresses and strains experienced by a specific layer (e.g., surface or base layer) vary from one pavement section to another. Hence, the stress/strain level delivered to any one pavement layer is a function of the material properties of that layer. This implies that while the AASHTO design procedure ensures that the global deflection of the pavement sections remains constant (item 1), the relative stress/strain magnitude delivered to each layer apparently is not. Thus, the results of the mechanistic analyses do not necessarily support the AASHTO layer coefficient or the AASHTO concept that the SN of the pavement is the sum of the SNs of its layers.
  - c) The tensile stress and strain induced at the bottom of the AC layer depend on the properties and thicknesses of all pavement layers. This implies that the AASHTO design procedure does not necessarily produce pavement sections with equal fatigue life. However, the global damage pavement response to compression in the pavement sections remains the same. Once again, the results of the mechanistic analyses do not support the present AASHTO layer coefficient concept.
2. For those pavement sections with the same layer properties but designed by the AASHTO procedure for various roadbed soils, the same traffic volume, and the same serviceability loss during an equal performance period, the mechanistic analyses indicate that the stresses, strains, and deflections induced in the pavements are not the same. This implies that the role of the resilient modulus of the roadbed soil in the AASHTO flexible pavement design equation needs to be investigated further and/or calibrated.
3. For those pavement sections with the same layer properties but different drainage coefficients that have been designed by the AASHTO procedure for the same roadbed soils, the same traffic volume, and the same serviceability loss during an equal performance period, the results of the mechanistic evaluations indicate the following:
  - a) The magnitude of deflections (amount of compression) experienced by the various pavement sections under a 9000-lb load varies from one pavement section to another. From these results it is surmised that the amount of damage experienced by each section will not be the same, and the loss of serviceability is not expected to be equal.
  - b) The magnitudes of the stresses and strains induced in the pavement sections and in each layer vary from one pavement section to another. From this it is postulated that

the amount of damage experienced by each pavement layer varies with the structure, and that the variability is expected to produce different losses of serviceability.

These two findings indicate that the role of the drainage coefficient (in adjusting the layer thicknesses) in the AASHTO design procedure may not be accurate. As a result, mechanistic calibration of the role of the drainage coefficient was undertaken. After several trials, the following mechanistic modifications in the role of the drainage coefficients in the AASHTO flexible pavement design procedures are recommended:

$$a_{ci} = (a_i)(m_i)^{0.5}$$

$$MR_{RBd} = (MR_{EFF})(m_3)^{0.5}$$

where

$a_{ci}$  = effective layer coefficient of layer  $i$

$a_i$  = layer coefficient of layer  $i$

$m_i$  = drainage coefficient of layer  $i$

$MR_{RBd}$  = design value of the resilient modulus of the roadbed soil

$MR_{EFF}$  = effective resilient modulus of the roadbed soil

$m_3$  = drainage coefficient of the subbase material or the layer immediately above the roadbed soil

This revision in the influence of the AASHTO drainage coefficients on the pavement design produces layer thicknesses is expected to insure that the amount of damage delivered to the pavement sections in terms of stresses, strains, and deflections is almost the same.

4. The effect of the drainage coefficient on pavement performance was also analyzed from a different perspective. Rather than using the drainage coefficient to decrease or increase the layer thicknesses, the effect of the quality of drainage on the service life of the pavement was assessed and presented in an easy-to-read nomograph. The method allows the pavement design engineer to analyze the cost and benefit of improving the drainage quality. This makes the effect of drainage quality on the pavement performance comparable with that for loss of serviceability due to environmental factors.
5. Results of the mechanistic evaluation of the AASHTO concept of loss of serviceability due to environmental factors indicate the following:
  - a) The AASHTO loss of serviceability concept is linear (the total loss of pavement serviceability is the sum of the loss of serviceability due to traffic and the losses due to swelling and frost heave potentials). The concept does not account for the interaction between the various serviceability losses. However, from the mechanistic viewpoint, the AASHTO concept seems to be reasonable.
  - b) The loss of serviceability due to environmental conditions could also possibly be expressed in terms of the effective roadbed resilient modulus.

## References

1. "American's Highway, Accelerating the Search for Innovation." Special Report 2020. Strategic Transportation Research Study: Highways. pp. 93-94. Transportation Research Board. National Research Council. Washington, D.C. 1984.
2. Strategic Highway Research Program, Research Plans. Final Report. pp. TRA2-6, Transportation Research Board. National Research Council, Washington. D.C. May 1986.
3. Strategic Highway Research Program. "Executive Summary, Report 1." prepared by the Texas Research and Development Foundation. November 1992.
4. *AASHTO Road Test, Report 5, Pavement Research*. Highway Research Board Special Report 61E. National Academy of Sciences - National Research Council Publication Number 954. Washington, D.C. 1962.
5. Irick, P. and W.O. Hadley. "An Approach to Improvements of Load Equivalence Factors from SHRP-LTPP Data." TRDF Technical Memorandum AU-204. Texas Research and Development Foundation. Austin, Texas. May 3, 1992.
6. Irick, Paul and William O. Hadley. "Pilot Study of the Effects of Materials and Construction Variabilities on Pavement Distress and Performance." TRDF Technical Memorandum AU-203. April 6, 1992.
7. Hadley, W.O. "Construction Variability Studies." TRDF Technical Memorandum AU-219. Texas Research and Development Foundation. Austin, Texas. October 16, 1992.
8. Hadley, William O. "Rutting Initiation Studies." TRDF Technical Memorandum AU-214. September 31, 1992.
9. Hadley, W.O. "Approach for Improving AASHTO Load Equivalence Factors Using SHRP-LTPP Data." TRDF Technical Memorandum AU-218. October 13, 1992.
10. Hadley, W.O. "PSI Estimates from SHRP Profilometer Roughness." TRDF Technical Memorandum AU-215. Texas Research and Development Foundation. Austin, Texas. October 12, 1992.
11. Hadley, W.O. "A Method of Estimating Serviceability Loss for Existing SHRP-LTPP Flexible Pavement Sections." TRDF Technical Memorandum AU-216. Texas Research and Development Foundation. Austin, Texas. October 12, 1992.
12. Hadley, W.O. "Traffic Data Assessment for the SHRP-LTPP Load Equivalence Factor Improvement Study." TRDF Technical Memorandum AU-217. Texas Research and Development Foundation. Austin, Texas. October 12, 1992.

13. SHRP-LTPP Manual for Profile Measurements. "Operational Field Guidelines Version 1.0." Operational Guide No. SHRP-LTPP-OG-005. December 1989.
14. "PASCO Film Interpretation Manual (PASCO-FMA)." Operational Guide No. SHRP-LTPP-OG-0024. May 1990.
15. Hadley, W.O. and M.G. Myers. "Rut Depth Estimates Developed from Cross Profile Data." TRDF Technical Memorandum AU-179. April 1, 1991.
16. Hadley, W.O. "Rut Depth Estimates from PASCO Cross Profile." TRDF Technical Memorandum AU-185. June 28, 1991.
17. *Data Analysis Work Plan, Long Term Pavement Performance Studies, SHRP Projects P-020A* Brent Rauhut Engineering Inc. and ERES Consultants, Inc. September 1990.
18. *SHRP Data Collection Guide.* Operational Guide No. SHRP-LTPP-OG-006. May 1990.
19. *Data Analysis - A Revised Research Plan - SHRP Project P-020B*, Michigan State University, September, 1990.
20. Rauhut, J. B. and M. I. Darter. "Early Analyses of LTPP General Pavement Studies Data." Executive Summary, Brent Rauhut Engineering, Austin, Texas, October 1993.
21. (Under development)---Data Processing and Evaluation.
22. Simpson, A. L., J. B. Rauhut, P. R. Jordahl, etal. "Sensitivity Analyses for Selected Pavement Distresses." Brent Rauhut Engineering, Austin, Texas.
23. Daleiden, J. S., J. B. Rauhut, B. Killingsworth, etal. "Evaluation of AASHTO Design Equations and Recommended Improvements." Brent Rauhut Engineering, Austin, Texas.
24. Daleiden, J. S., J. B. Rauhut, B. Killingsworth, etal. "Lessons Learned and Recommendations for Future Analyses of LTPP Data." Brent Rauhut Engineering, Austin, Texas.